

**The functional role of MITF in DNA damage
response pathways and its potential modulation of
the immune system by regulating NFκB
phosphorylation**

Dissertation

With the aim of achieving a doctoral degree at the Faculty of Mathematics,
Informatics and Natural Sciences
Department of Biology
of Universität Hamburg

Submitted by

Diploma biologist
Laia Pagerols Raluy
Born in Manresa

Hamburg, September 2013

Genehmigt vom Fachbereich Biologie
der Fakultät für Mathematik, Informatik und Naturwissenschaften
an der Universität Hamburg
auf Antrag von Professor Dr. M. HORSTMANN
Weiterer Gutachter der Dissertation:
Priv.-Doz. Dr. H. LÜTHEN
Tag der Disputation: 08. November 2013

Hamburg, den 24. Oktober 2013

A handwritten signature in blue ink, consisting of a stylized 'L' followed by a horizontal line and a small flourish.

Professor Dr. C. Lohr
Vorsitzender des
Fach-Promotionsausschusses Biologie

To my father, who taught me to live with purposefulness, commitment and devotion.

("Pit i collons!")

TABLE OF CONTENTS

1	INTRODUCTION.....	1
1.1	Melanocytes	1
1.1.1	Genomic stability	1
1.1.2	Pigmentation	2
1.1.3	Immune system in the skin	3
1.2	Malignant melanoma	4
1.2.1	Molecular biology	5
1.2.2	Therapy	5
1.3	MITF.....	6
1.3.1	MITF-M.....	7
1.3.2	MITF-M regulation	8
1.3.3	MITF-M and melanoma	9
1.4	XPG and ATM in the role of DNA damage repair.....	10
1.5	NFκB	10
1.5.1	p65	12
1.5.2	p65 regulation.....	13
1.5.3	p65and melanoma.....	15
1.6	Aim of the study.....	16
2	MATERIALS AND METHODS	17
2.1	Materials.....	17
2.1.1	Chemicals	17
2.1.2	Kits	17
2.1.3	Cell culture media and reagents	17
2.1.4	Reagents for molecular biology methods.....	18
2.1.5	Reagents for protein chemical methods.....	18
2.1.6	Buffers.....	18
2.1.7	Oligonucleotides.....	20
2.1.7.1	Primers.....	20
2.1.7.2	siRNA	21
2.1.8	Antibodies	21
2.1.9	Equipment	22
2.1.10	Plastic ware.....	23
2.2	Methods	23
2.2.1	Cell biology methods	23
2.2.1.1	Cell culture	23
2.2.1.2	UV Exposure/ γ -irradiation	23
2.2.1.3	Treatment with kinase inhibitors and cytostatics	24
2.2.1.4	Transfection with siRNA	24
2.2.2	Molecular biology methods	24
2.2.2.1	Apoptosis assay	24
2.2.2.2	Cell cycle analysis	25
2.2.2.3	DNA damage repair analysis	25
2.2.2.3.1	UV- induced DNA lesions	25
2.2.2.3.2	Cisplatin- induced DNA lesions	25
2.2.2.4	RNA isolation.....	26
2.2.2.5	cDNA synthesis	26
2.2.2.6	Real time PCR.....	27
2.2.3	Protein chemistry methods	28

TABLE OF CONTENTS

2.2.3.1	SDS-PAGE (SDS-polyacrylamide gel electrophoresis) - WB (Western blot)	28
2.2.3.2	Immunocytofluorescence (IF)	30
2.2.3.3	ELISA (Enzyme Linked Immunosorbent Assay)	31
3	RESULTS	32
3.1	MITF is involved in the repair of DNA lesions induced by UV irradiation and cisplatin treatment	32
3.2	MITF´s role in DNA damage repair under UVB irradiation is partially mediated through the regulation of XPG	36
3.3	The regulation of XPG by MITF is DNA lesion specific	39
3.4	The role of MITF in the DNA damage response under UVB exposure is also mediated by the regulation of ATM	41
3.5	In UV irradiated melanoma cells phosphorylation of Ser85- NEMO is mediated by ATM	43
3.6	MITF regulates the NFκB pathway by transactivation of ATM.....	44
3.6.1	Transcriptional transactivation of NFκB is not dependent on MITF	44
3.6.2	MITF is involved in the activation of NEMO and p65 proteins under UVR.....	46
3.7	MITF plays a role in the secretion of IL8 and IL10 by regulating the.....	52
4	DISCUSSION	56
4.1	Nucleotide excision repair capacity of primary melanocytes and melanoma cells is dependent on MITF	56
4.2	MITF controls DDR by direct transcriptional regulation of XPG in a lesion-.....	57
4.3	MITF regulates ATM upon UV irradiation.....	58
4.4	Regulation of NFκB (p65) activation by MITF is partially dependent	58
4.5	Expression of IL-8 and IL-10 is negatively regulated by MITF	60
5	SUMMARY	62
6	ZUSAMMENFASSUNG	63
7	LIST OF ABBREVIATIONS	64
8	REFERENCES.....	67
9	EIDESSTATTLICHE ERKLÄRUNG	74
10	BESTÄTIGUNG DER SPRACHLICHEN KORREKTHEIT DURCH „NATIVESPEAKER“	75
11	ACKNOWLEDGEMENTS	76

1 INTRODUCTION

The skin is the largest organ of the body and represents a physical barrier to the environment. This barrier defends against potential damaging factors such as microorganisms, external injuries and toxic agents.

The major source of DNA damage in skin cells is ultraviolet radiation (UVR). In response to this threat, cells use a specific DNA damage repair mechanism in which UV damaged bases are removed as an oligonucleotide fragment; this is the so-called nucleotide excision repair (NER). Additionally, melanocytes in the epidermis produce melanin which forms a shield over the nuclei of the neighboring cells and the melanocytes themselves, thus protecting them from UV-induced DNA damage. UV exposure may also lead to skin inflammation, which is initiated by keratinocytes and melanocytes, and executed by the immune cells of the epidermis and dermis.

1.1 Melanocytes

Upon melanocytic differentiation, melanoblast precursors migrate from the neural crest to a designated location, which can be the uvea[1], inner ear[2], heart[3] or the basal layer of the epidermis. Melanocytes are characterized by a low proliferation rate and an enormous resistance towards apoptosis [4]. In addition to the role in the pigmentation process, melanocytes are also defined as stress sensors [5] and skin's immune system response mediators [6].

1.1.1 Genomic stability

Skin cells are continuously submitted to genotoxic factors which compromise the integrity of their DNA. Since melanocytes are crucial to the protection of the cellular milieu upon UV radiation, the genomic stability of these cells must be ensured. Metabolic processes, chemical agents and ionizing radiation may induce oxidation, alkylation, hydrolysis or deamination of single nucleotides, which are repaired in the majority of cases by the base-excision repair (BER) system [7]. An additional DNA damage repair mechanism is the nucleotide-excision repair (NER) system, which is responsible for those DNA damages that entail structural changes of the double helix. As such, bulky DNA adducts (cyclobutane pyrimidine dimers (CPD) and pyrimidine (6-4) pyrimidone photoproducts (6-4PP) are caused by UV radiation. Furthermore, chemotherapeutic agents such as platinum derivatives may also partially activate this pathway [8]. NER consists of two separate pathways: (I) transcription-coupled NER

(TC-NER), restricted to actively transcribed genes, and (II) global genomic NER (GG-NER), which covers the whole genome. As shown in Figure 1, both pathways only differ in the DNA lesion recognition [9].

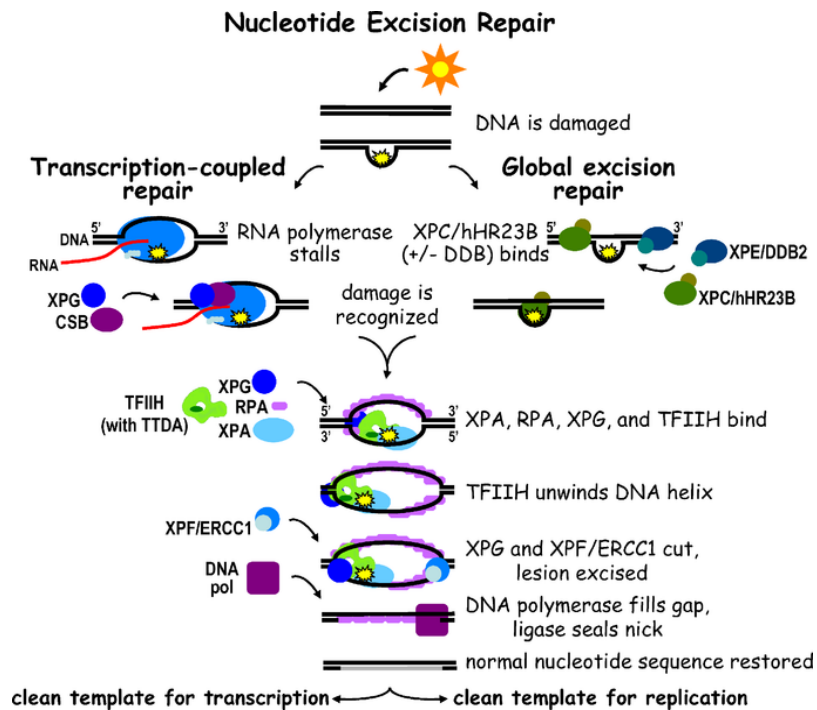


Figure 1. Nucleotide excision repair. Molecular description of the TC- and GG-NER pathways. Adapted from Fuss et al., PLoS Biol., 2006[9].

NER follows a three- step process in which the DNA damage is recognized, subsequently excised and finally the missing DNA fragment is newly synthesized using the complementary DNA strand as a template.

Under severe stress conditions, such as ionizing radiation or treatment with certain types of chemotherapeutics, including cisplatin, carboplatin and etoposide, DNA double-strand breaks (DSB) can occur. In this case, no complementary DNA strand can be used for the repair of the damaged DNA, thus potentially leading to chromosomal rearrangements. The cell utilizes one of three mechanisms to repair DSBs: homologous recombination (HR), non-homologous end joining (NHEJ) and microhomology-mediated end joining (MMEJ).

1.1.2 Pigmentation

Pigmentation is the skin's photoprotective mechanism, which ensures the genomic stability of the cells upon UVR; this process requires the participation of different cell types in which the melanocytes are responsible for the production of melanin

(melanogenesis). Skin pigmentation can be constitutional (basal) or UVR-induced (tanning). In both cases, keratinocytes turn on the expression of α -melanocyte stimulating hormone (α -MSH) and other peptides by processing the precursor protein pro-opiomelanocortin (POMC) [10]. Subsequently, α -MSH is secreted and binds to the melanocortin 1 receptor (MC-1R) present on the melanocytes' surface leading to an increase of cyclic adenosine monophosphate (cAMP). Concomitantly, the expression of the Microphthalmia-associated transcription factor (MITF) is induced resulting in an upregulation of tyrosinase [11] and tyrosinase related proteins -1 and -2 (TYRP-1 and -2) [12]. These enzymes will then synthesize melanin which will be transferred into the surrounding keratinocytes (See Figure 2).

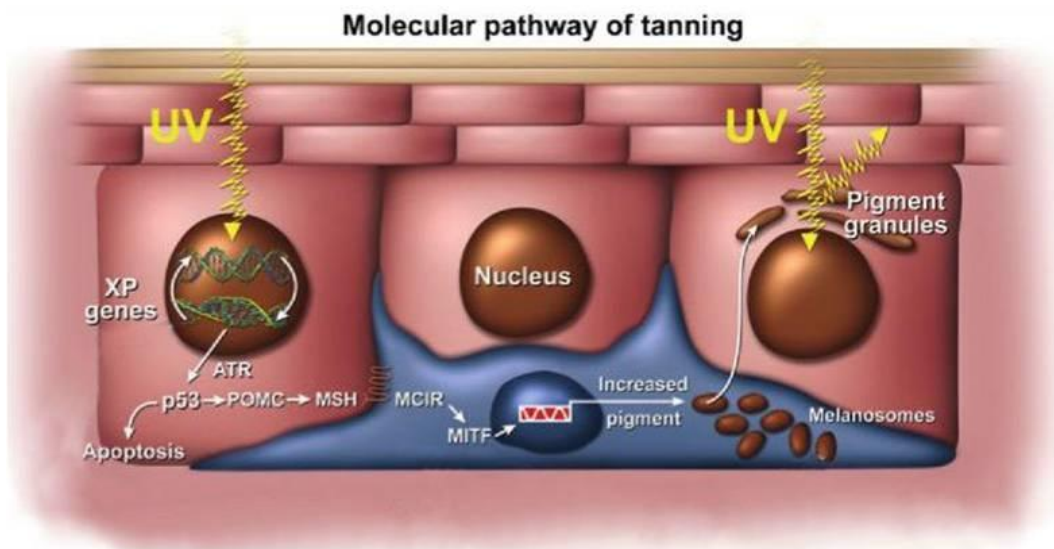


Figure 2. UV-induced pigmentation process. Adapted from Miller, A. J. and Tsao, H.Br J Dermatol, 2010 [13].

Pigmentation underlies a complex regulation in which many factors play an important role, for instance, (I) dendricity of the melanocytes, (II) tyrosinase activity and (III) single nucleotide polymorphism (SNP) of the MC-1R [14-16].

Additional functions including apoptosis, DNA damage repair and inflammation have been attributed to α -MSH [17]. In the past, several groups were able to show an enhanced UV-induced DNA repair capacity of keratinocytes and melanocytes when α -MSH treatment preceded UV exposure. In addition, these data were complemented by an analysis demonstrating an induction of the NER system in those cells in which the melanocortin peptide was applied [18].

Finally, α -MSH shows prominent anti-inflammatory effects by antagonizing pro-inflammatory cytokines, such as interleukin (IL-1, IL-6) and tumor necrosis factor- α (TNF- α), indicating a role of this hormone in the regulation of the immune system [19].

1.1.3 Immune system in the skin

Previous observation of different immune cell populations distributed along the epidermis and dermis suggested the skin's role in the immunological response to different stimuli. The epidermis hosts Langerhans cells (LCs), which are specialized dendritic cells (DCs), and intraepithelial lymphocytes. Further below in the dermis, reside dendritic cells, mast cells and memory T cells (See Figure 3).

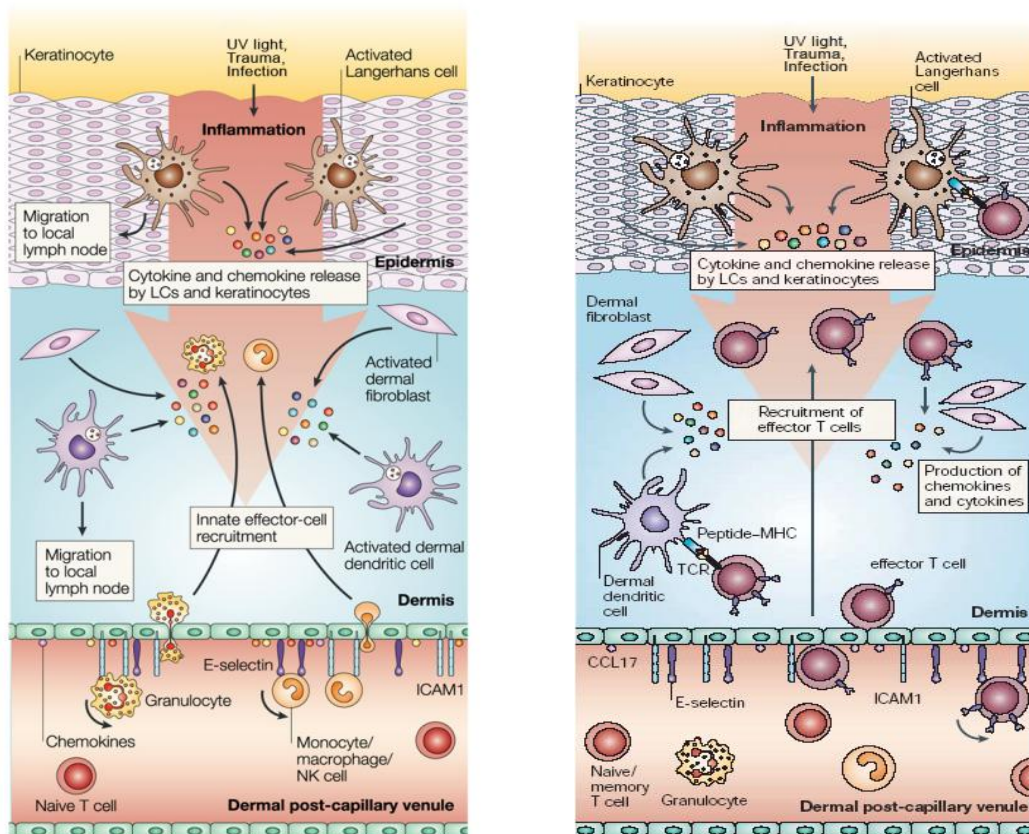


Figure 3. Immune mechanisms in the skin. Exposure of the skin to various stimuli such as UVR, trauma or infection, leads to the activation of pathways involving cells of the innate (left) and adaptive (right) immune system. Adapted from Thomas S. Kupper & Robert C. Fuhlbrigge, *Nature Reviews Immunology*, 2004[20].

In past decades, numerous studies demonstrated the crucial participatory function of the melanocytes in the cutaneous immune response. Upon genotoxic stress, including UVR, melanocytes, as well as keratinocytes and LCs, release different pro-

inflammatory cytokines, including IL-1, TNF- α , IL-10 and chemokines, such as, IL-8 [21-25]. The expression of these immune factors is primarily regulated by NF κ B (nuclearfactor kappa-light-chain-enhancer of activated B cells), specifically by the p65/p50 heterodimer [26-30]. In addition to its implication in pro-inflammatory processes, angiogenic properties have been assigned to IL-8. This chemokine has been shown to be overexpressed in metastatic melanoma, which may partially account for its invasiveness. Notably, although IL-10 is commonly considered an anti-inflammatory cytokine, Scholzen et al. observed a pro-inflammatory function of IL-10 in UV-irradiated microvascular endothelial cells, which showed a UV-induced upregulation of IL-6 and IL-8 in dependence of IL-10 [31].

1.2 Malignant melanoma

Malignant melanoma is by far less frequent than basal cell and squamous cell carcinoma, but it accounts for 75% of all deaths caused by skin cancer [32]. Since recognition of melanoma at an early stage is crucial for patient survival, an adequate staging diagnosis has been developed over the past years. In earlier diagnostic procedures the Clark level, in which the invasion of the melanoma along the skin is analyzed, was utilized as staging system [33]. However, due to the low precision of this measurement, the Clark level system was combined with the Breslow level, which measures tumor thickness [34], for better prognostic power.

The main cause of melanoma is the repeated exposure to UV radiation, sunburns exhibiting a higher risk when compared to tanning. Other predisposing factors, such as pigmentation and genetic alterations, are highly relevant in the development of malignant melanoma [35-36].

1.2.1 Molecular biology

Melanoma arises from the transformation of melanocytes and occurs in any area where the pigment-producing cells are located, usually in the skin (cutaneous melanoma). Despite the high genetic heterogeneity found in melanoma, common signaling pathways involved in survival, proliferation, apoptosis and DNA damage response are affected. The most recurrent mutations occur in the RAS/RAF/MAPK pathway, which is involved in survival and proliferation. This leads to hyperactivation of the signaling cascade. Many studies reveal genetic aberrations of the *RAS* and *RAF* genes (Q61R N-RAS and V599E B-RAF mutations) but since these mutations

occur in only 26% and 42% of cutaneous melanomas, respectively [37-38], alterations in other genes must co-occur. In line with this notion, point mutations in the mitogen activated kinase (MAPK) family have been described [39].

Furthermore, a relevant pathway in melanoma is the PI3K/AKT/mTOR signaling, which is responsible for survival, proliferation, motility and invasion. Most of the mutations in this pathway rely on a loss of function of phosphatase and tensin homolog protein (PTEN), an inhibitor of the cascade, or on activating mutations in the (phosphatidyl-inositol-3 kinase) *PI3K* and *AKT* genes [40-41].

Additionally, gene aberrations in hereditary but also sporadic melanomas are located in the *CDKN2A* (Cyclin-dependent kinase inhibitor 2A) gene, which encodes for the p16^{INK4A} and p14^{ARF} proteins [42-43]. Both products are responsible for the promotion of the cell cycle arrest, the former inhibiting cyclin- dependent kinases (CDKs) and the latter inducing p53 activity. In some other cases, genetic defects in *CDK4* and *TP53* genes have been reported [44-45].

In addition, mutations in genes implicated in the DNA damage repair machinery, as observed in *xeroderma pigmentosum* (XP) patients, and genetic variability of the MC-1R resulting in pigmentation heterogeneity [46-47] are well-known risk factors in melanomagenesis beside sun exposure.

1.2.2 Therapy

A surgical removal of the tumor will increase the chance of survival, only in those cases, in which melanoma is detected at its early stages. By contrast, diagnosis of advanced and metastasized melanoma leads to a dramatically decreased prognosis with a median overall survival of only about 8% [48-49].

A common strategy treating advanced melanoma is the usage of DNA damaging agents such as platinum-containing drugs, including carboplatin and cisplatin, which lead to intrastrand and inter-strand DNA crosslinks. Further promising drugs in the treatment of metastatic melanoma are dacarbazine, an alkylating agent, and nab-paclitaxel, a tubulin-blocking drug. Comparative studies in patients with metastatic melanoma treated with dacarbazine or nab-paclitaxel, showed a higher overall response rate and a lower rate of progressive disease for the latter [50].

In addition to the conventional cytotoxic therapies immunological treatments with IL-2 and interferon- α (IFN- α) as adjuvants have been attempted yet showing limited success [51]. Recently, more rational treatment strategies have been tested targeting

oncogenic pathways more specifically. As such vemurafenib, a second generation BRAF-inhibitor drug demonstrated high response success albeit rapid resistance and early relapse of melanoma was observed [52-54]. Lately, MEK inhibitors are being tested and show some promise in the treatment of metastatic melanoma [55].

1.3 MITF

The human *MITF* gene is located on chromosome 3p12.3- 14.1 and encodes a basic helix-loop-helix zipper (b-HLH-Zip) transcription factor[56]. Due to its structural homology to c- myc, MITF belongs to the Myc supergene family and binds to DNA either as a homodimer or a heterodimer together with transcription factors of the same group (MiT family), the so called transcription factors –B, -3 and –C (TFEB, TFE3 and TFEC, respectively). MITF binds to the promoters of the target genes through E- box sequences: canonical CACGTG and non-palindromical CACATG [57]. So far, nine isoforms have been identified, which share nine exons and differ in the first one thereby activating nine distinct promoters (Figure 4) [12].

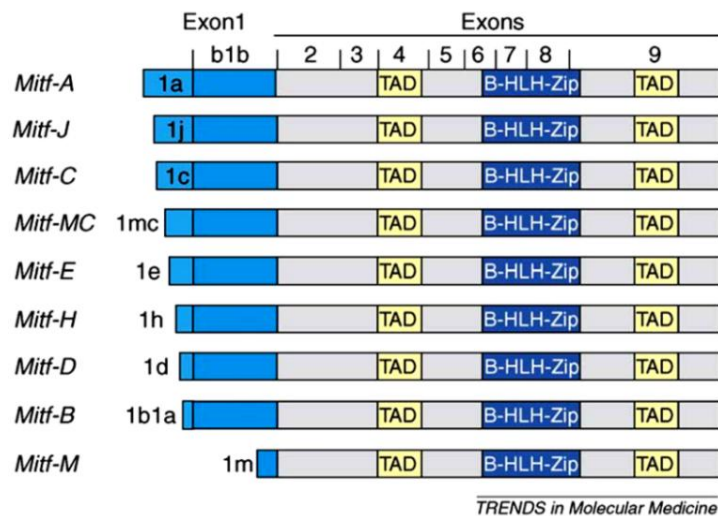


Figure 4. MITF isoforms. Transcription of the MITF gene may result in one of the nine isoforms. All of them express exons 2-9, where the transactivation domain (TAD) and the b-HLH-Zip are located, and an isoform-specific exon 1. Adapted from Levy, C., M. Khaled, and D.E. Fisher. Trends in molecular medicine, 2006 [12].

Generally, MITF isoforms are expressed in several tissues. MITF-A, for instance, which can be found in bone and kidney. MITF-D is mostly expressed in retinal pigment epithelium (RPE), osteoclasts and macrophages. By contrast, the isoforms MITF-M and MITF-MC are selectively expressed in melanocytes and mast cells, respectively [58].

1.3.1 MITF-M

As outlined above, the melanocyte-specific MITF-M plays a crucial role in the development and migration of melanoblasts from the neural crest to other sites of the body during embryogenesis [59]. Additionally, analyses in inherited human disorders, such as Waardenburg syndrome type IIA (WS2A) and Tietz syndrome were associated with MITF mutations [60]. These auditory and pigmentary defects can be explained by a melanocytic deficiency in the inner ear and skin, elucidating further functions of MITF, including differentiation, pigmentation, survival and proliferation. Accordingly, *BCL-2*, a gene encoding for the anti-apoptotic protein BCL-2, is directly regulated by MITF-M, as well as the transcriptional activity of *p16^{INK4A}* [61-62]. Furthermore, the MITF regulation of the pigmentation process relies on the regulation of genes involved in melanogenesis, such as *TYR* and *TRYP1*. In the past, several studies proposed a role of MITF in inflammation. In 2011, Bertolotto et al., concomitantly to Yokoyama and coworkers, identified a SUMO-defective form of MITF with potential regulatory activity on inflammatory genes such as *IL-6*, *CCR7* (C-C chemokine receptor type 7) and *IRAK-2* (*IL-1 receptor-associated kinase-like 2*) [63-64]. Additionally, a novel function for MITF in the DNA damage response has been hypothesized implicating a regulatory role in DNA damage repair [65].

1.3.2 MITF-M regulation

MITF expression and activation can be regulated by several signaling pathways (Figure 5). At the transcriptional level, MITF upregulation is triggered by α -MSH and Wnt pathways. As described above, UV-irradiated keratinocytes secrete α -MSH, which binds to MC-1R resulting in an increase of cAMP levels. High concentrations of cAMP lead to activation of PKA and subsequent phosphorylation of the cAMP responsive element binding protein (CREB). Activation of CREB entails recruitment of the CREB binding protein (CBP), thereby binding as a protein complex to the cAMP responsive element located in the promoter of the *MITF* gene [66-67].

Alternatively, Wnt activates the corresponding receptor Frizzled inhibiting the glycogen synthase kinase-3 β (GSK-3 β), leading to an increase of β -catenin, which will then translocate into the nucleus. Once there, β -catenin binds to LEF/TEF family transcription factors activating genes with promoters containing LEF-binding sites, such as *MITF* [68]. Additionally, based on in vitro protein-protein binding studies, Saito et al. demonstrated an MITF-M self-regulatory capacity by acting as co-factor

for LEF-1 [58]. Additional factors found to directly increase the transcriptional activity of MITF were the transcription factors SOX10 and PAX3, which lead, when mutated, to the development of the Waardenburg syndrome type I and III, and type IV, respectively [69-71].

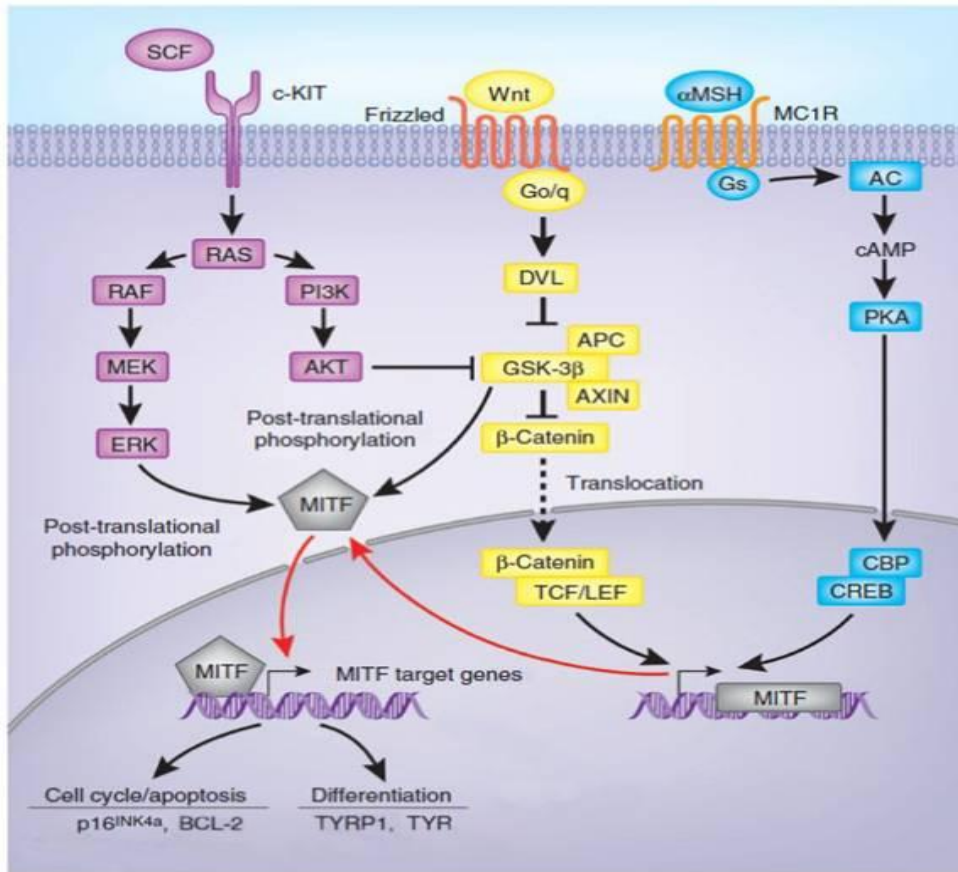


Figure 5. MITF regulation in melanocytes. The three main MITF regulatory pathways. Adapted from Hocker et al. J Invest Dermatol, 2008 [66].

Additionally, MITF-M can be modulated through post-translational changes. The c-KIT signaling pathway accounts for such regulation. After binding of this receptor tyrosine kinase to its ligand stem cell factor (SCF), two major pathways are activated, the MAPK- and the PI(3)K-cascade, among others. On the one hand, MAPK induction leads to the phosphorylation of MITF at the Ser 73 and Ser 409 through the activation of ERK-2 and p90RSK (90 KDa ribosomal S6 protein kinase), respectively. The dual phosphorylation of MITF protein results in its ubiquitination and thus, degradation [72], whereas the single phosphorylation at the Ser 73 site leads to increased MITF transcriptional activity [73]. On the other hand, the triggering of PI(3)K signaling leads to inactivation of GSK-3 β , which accounts for the induction of MITF transcriptional activity through its phosphorylation at ser298 [74]. As mentioned

above, a novel activating mutation (SUMO-defection) of MITF concerning amino acid 318 has recently been identified [63-64].

1.3.3 MITF-M and melanoma

Garraway and coworkers identified amplifications at the MITF locus in about 20% of metastatic melanomas and in melanoma cell lines among an NCI panel panel of 60 cancer cell lines compared to normal cells, suggesting MITF as a lineage-specific oncogene [75]. Furthermore, Bertolotto et al. were able to identify a novel germ line mutation which impaired SUMOylation of MITF leading to a higher risk in developing melanoma and renal cell carcinoma (RCC) [63-64].

Nevertheless, a dual role has been assigned to MITF in the past years. Studies demonstrated that the transcriptional activity of genes yielding proteins responsible for cell cycle arrest, such as cyclin dependant kinase inhibitor (CDKN1A) and p16^{INK4A}, was positively regulated by MITF. Moreover, further studies described different cellular populations within a melanoma regarding MITF expression level. High MITF-expressing cell subpopulations acquire proliferative features, as reflected by the activation of DNA damage repair system and DNA replication. By contrast, those cell populations in which MITF expression is low, invasiveness override the proliferation signature, at the expense of an increased genomic instability. Additionally, low MITF expression leads to the upregulation of genes inducing metastasis, such as *BMP4* (bone morphogenetic protein 4) and *SHC4* (Src homology 2 domain containing) [65, 76]. In this molecular model, proliferative and invasive phenotypes would be switchable depending on the microenvironment, probably assigned to hypoxia and inflammation, among others [65, 77].

1.4 XPG and ATM in the role of DNA damage repair

As outlined above, UV-induced lesions are mainly corrected by the NER system albeit HR repair mechanisms, which are responsible for the repair of DSBs may be activated as well.

XPG (xeroderma pigmentosum complementation group G) is also known as excision repair cross-complementing, rodent repair deficiency, complementation group 5 (ERCC5) and is the endonuclease responsible for the 3' incision in damaged DNA upon UVR. XPG belongs to the NER machinery operating in TC-NER as well as GG-NER (see Figure 2). Furthermore, XPG is also involved in transcription by RNA pol II,

as a binding partner of TFIIH (general transcription factor II H polypeptide 2) [78]. Mutations in *XPG* cause xeroderma pigmentosum (XP), a disease characterized by a hypersensitivity to UV irradiation and a high susceptibility to develop skin cancer upon UV exposure [79]. *XPG* aberrations affecting its binding affinity to TFIIH lead to Cockayne syndrome (CS) which is characterized not only by severe deficiencies in the nucleotide excision repair system, but also in transcriptional activity [80]. CS patients exhibit a neurological dysfunction, which includes light sensitivity and osteoporosis [81].

ATM (ataxia telangiectasia mutated) is considered a DNA damage sensor. It is a serine/threonine protein kinase and member of the PIKK (phosphatidylinositol 3' kinase-like kinase) family. Upon genotoxic stress such as UV radiation, ATM undergoes a series of phosphorylations which leads to the activation of proteins involved in apoptosis, cell cycle arrest, DNA damage repair and inflammation, such as p53, Chk2 and NEMO (NF κ B essential modulator) [82-86]. Mutations in the *ATM* gene result in the autosomal recessive disease ataxia telangiectasia (AT). Patients affected by this disorder manifest neural degeneration, high sensitivity to radiation and increased risk to develop cancer [87].

1.5 NF κ B

NF κ B is a family of ubiquitous “early-activating” transcription factors consisting of five members classified in two subgroups, class I (or NF κ B subgroup) and class II (or Rel subgroup), according to their C-terminal structure. The NF κ B proteins p105 and p100, precursors of p50 and p52, respectively, contain an ankyrin-repeating region (ANK) that functions as a transrepression domain. The Rel subgroup is characterized by a transactivation domain (TAD) and is composed of the RelA (p65), RelB and c-Rel proteins. All proteins of the NF κ B family share a Rel homology domain (RHD) with DNA/I κ B-binding and dimerization features (Figure 6).

The Rel proteins can form homo-dimers or hetero-dimers with members of the NF κ B subgroup, leading to activation of the pathway. By contrast, NF κ B-protein homo-dimerization results in a signaling repression [88].

Once dimerization of NF κ B subunits takes place, the protein complex will bind to specific DNA binding sites (κ B sites) which present high variability in the sequence and a different specificity for each dimer composition, leading to a differential transcriptional regulation.

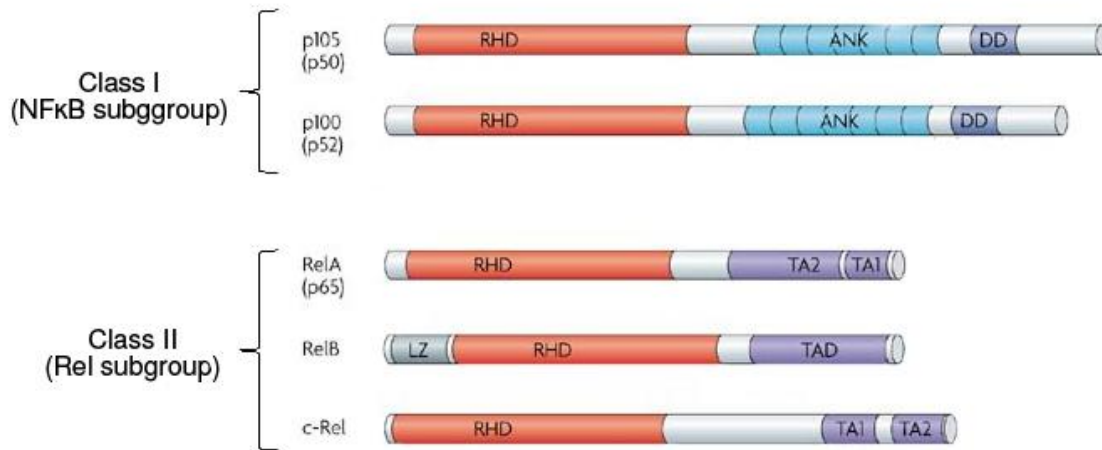


Figure 6. NFκB family members. The NFκB family is divided in two subgroups. Class I is represented by p105 and p100, which under controlled proteolysis result in p50 and p52, respectively. To the class II subgroup belong RelA (also termed p65), RelB and c-Rel. Both classes present a Rel homologous domain (RHD) but differ in the ankyrin-repeating region (ANK) and the transactivation domain (TAD; TA1 and TA2, subdomains of TAD); LZ, putative leucine-zipper-like motif; DD, death domain homology region. Adapted from Neil D. Perkins. Nature Reviews Molecular Cell Biology, 2007 [89].

1.5.1 p65

Although there is a high variability in hetero- and homodimerization, the term NFκB usually refers to the p65 and p50 heterodimer (hereafter called NFκB). In the past, the relevance of NFκB to the immune response has been established by the identification of target genes encoding for cytokines, chemokines and adhesion molecules such as IL-6, IL-2, IL-8, TNF-α and ICAM-1[90]. Analyzing the molecular biology of diverse immune disorders, NFκB has been shown to be activated in a series of inflammatory diseases, including rheumatoid arthritis, asthma and inflammatory bowel disease [91-93]. Furthermore, several studies on virus-related diseases demonstrated an activation of NFκB after infection, leading to the regulation of viral DNA replication, cell cycle and cellular apoptosis [94-95], which may be explained by the activation of certain target genes, such as BCL-2, CD95 and CDKN1A (p21^{CIP1}). In the past years, an increasing interest in NFκB in the DDR context has been emerging. As reviewed by Janssens and Tschopp, NFκB differs in its activation or repression potential depending on the applied genotoxic stimulus [96].

1.5.2 p65 regulation

NFκB is regulated by a variety of different stimuli. In general, three NFκB pathways have been described (Figure 7).

The first one, the so-called canonical pathway, is triggered by proinflammatory cytokines and pathogens, including TNF-α, IL-1 and LPS, among others, and leads to the activation of the p65/p50 heterodimer. Under non-activating conditions, the heterodimer is constitutively inhibited by IκBα (nuclear factor of kappa light polypeptide gene enhancer in B-cells inhibitor, alpha), which binds to NFκB thereby masking the nuclear localization signal (NLS) and thus impeding the translocation of NFκB into the nucleus. Upon stimulation, IKK (IκBα kinase) signalosome is activated, leading to the phosphorylation, ubiquitination and subsequent degradation of IκBα, which in turn, results in nuclear accumulation of NFκB. The IKK protein complex consists of two kinases (IKKα and IKKβ) and a regulatory subunit (NEMO, NFκB essential modifier), responsible for the recruitment of IKKα and IKKβ [88].

On the other hand, a non-canonical pathway has been recently identified. Here, the activated NFκB complex comprises the p52 and RelB subunits. After binding of TNFR family ligands, such as BAFF (B-cell-activating factor of the tumor necrosis factor) and CD40, to the corresponding receptor, activation of NIK (NF-κB-inducing kinase) occurs. Subsequently, an IKK complex exclusively formed by IKKα dimers is phosphorylated, thereby inducing the proteolysis of p100 protein into p52. Finally, RelB and p52 dimerize and migrate into the nucleus [88].

The third pathway is induced by a variety of stimuli related to DNA damage and exhibit a late and weak activation of NFκB. Among those, two kinds of regulatory mechanisms are distinguished, one being activated by the majority of genotoxic factors and merging into the canonical pathway, and a second one triggered by UVR and featured by an IKK-independent signaling. A possible mechanism for the activation of NFκB under UV exposure may be, on the one hand, the clustering of IL-1R or TNF-R and subsequent activation of the pathway or, on the other hand, the release of a signal from within the cell. Indeed, some reports suggest the activation of NFκB (p65/p50) following DNA damage [97-98]. As mentioned above, UVR leads to ATM phosphorylation and activation, which in turn, binds to and phosphorylates NEMO at serine 85, leading to its translocation into the cytoplasm. Once there, NEMO allows the formation of the IKK signalosome thereby inducing NFκB [96].

Nevertheless, activation of NF κ B not only relies on the nuclear localization of the transcription factor, but also on post-translational modifications, as acetylation, methylation, ubiquitination and phosphorylation, the latter occurring in the cytoplasm as well as in the nucleus. A well-defined p65 phosphorylation site is the serine 536 (S536), which is targeted by various kinases, including the IKKs, exhibiting an increased transcriptional activity, probably caused by a conformational modification of the protein [99].

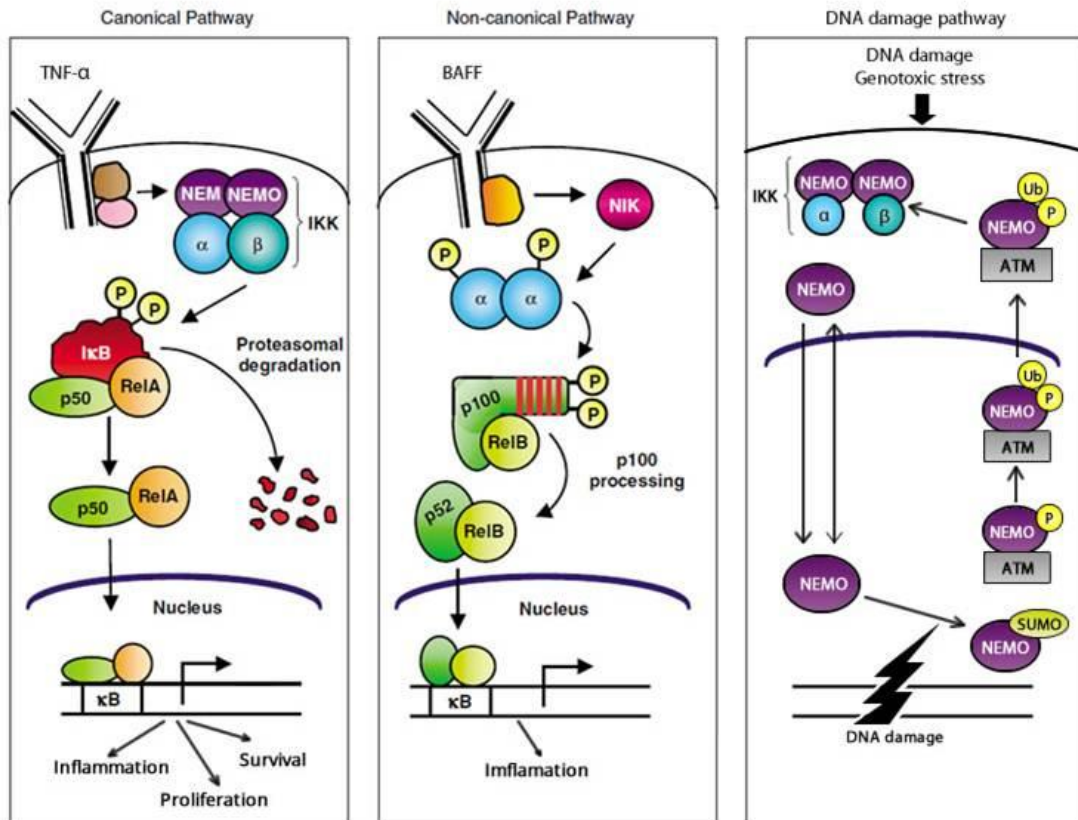


Figure 7. Three NF κ B pathways. Activation of the canonical pathway implies recruitment and activation of the IKK signalosome (IKK α , IKK β and NEMO) following phosphorylation (P), ubiquitination and subsequent degradation of I κ B. Thus, NF κ B (comprised by p50 and p65 subunits) is freed and migrates to the nucleus. The non-canonical pathway differs in, (i) the NF κ B complex, represented by the p52 and RelB proteins, and (ii) the kinases responsible for its activation, namely NIK, which activates IKK α dimers. The third pathway is triggered by DNA damage. In this case, DNA lesions caused by genotoxic agents, such as UVR, lead to ATM activation and subsequent phosphorylation of NEMO. After several post-translational modifications, such as ubiquitination (Ub), NEMO translocates to the cytoplasm, releases from ATM and recruits IKK α and IKK β . p100, precursor of p52. Adapted from Gilmore T. D. *Oncogene*, 2006 [88].

1.5.3 p65 and melanoma

In the past, numerous studies demonstrated a key role of NFκB in malignant melanoma. Melanoma progression has been attributed to dysregulated activation of NFκB [100]. Accordingly, Dhawan and Richmond observed a higher NFκB upregulation in human melanoma lesions compared with cutaneous melanocytes [101]. Hence, several genetic aberrations affecting cellular proliferation and apoptosis are responsible for increased NFκB transcriptional activity. In line with this notion, it has been observed that mutations in *p16^{INK4A}* and *p14^{ARF}* genes result in an upregulation of p65 activity [102-104]. Similarly, activating mutations in N-RAS and B-RAF genes result in a hyper-activation of ERK1/2 which, in turn, leads to an increased NFκB transcriptional activity. Furthermore, previous studies have described that PTEN dysfunction results in a higher activation of AKT, which leads to the phosphorylation and thus, activation of IKKα and NFκB (p65) [51]. Additionally, NFκB shows an auto-activation loop, thereby increasing the transcriptional rate of genes, the translational products of which trigger signaling cascades with a final NFκB activation. This is the case for cytokines and chemokines, such as IL-1, IL-8 and RANTES (Regulated on Activation, Normal T cell Expressed and Secreted) [105-107]. Bloethner and coworkers, for instance, suggest a cytokine and chemokine-mediated NFκB activation following RAS and RAF mutations in several melanoma cell lines and melanoma [108].

As described by several groups, increase of activated NFκB results in upregulation of target genes responsible for a broad spectrum of biological functions including anti-apoptosis, survival, proliferation, inflammation and invasion, promoting a highly aggressive melanoma phenotype, as shown for instance by a decrease of angiogenesis in murine metastatic melanoma after down regulation of NFκB [109].

1.6 Aim of the study

MITF-M is a transcription factor specifically expressed in melanocytes and amplified in about 10% and 20% of primary cutaneous and metastatic melanomas, respectively. In addition to its role in survival, proliferation and differentiation, MITF accounts for genomic stability and, as recently suggested, for the modulation of invasive and inflammatory processes in malignant melanoma.

The goal of this project was to investigate a potential impact of MITF on the DNA damage repair capacity of melanocytes and melanoma cells exposed to a variety of genotoxic procedures such as UVR and cisplatin treatment. The mechanistic basis of MITF's role in such DNA damage response pathways had to be determined.

A further objective of the present work was to explore a functional link between MITF and NF κ B in response to UV exposure. Previous data suggested a direct transcriptional regulation of the DNA damage sensor protein ATM by MITF. In turn, ATM activates NEMO, which is the master regulator of the NF κ B subunit p65. In analogy to MITF, NF κ B plays a crucial role in proliferation and survival, and it is also involved in DNA damage response signaling. Consequently, the activity of the canonical NF κ B pathway was studied under modulation of MITF expression and genotoxic UVR. Given the NF κ B-mediated regulation of cytokines and chemokines, we asked whether MITF might indirectly affect inflammatory response pathways induced by genotoxic stress.

Studies on the functional impact of MITF on DNA damage repair processes and inflammatory reactions after genotoxic attack may provide significant insights into protective mechanisms of the melanocytic lineage, which upon transformation could help to explain the enormous treatment resistance and the notorious escape from immunological surveillance of melanoma cells.

2 MATERIALS AND METHODS

2.1 Materials

2.1.1 Chemicals

Standard chemicals and solvents were purchased from Bio-Rad (München, Germany), Carl Roth (Karlsruhe, Germany), Invitrogen (Darmstadt, Germany), Merck (Darmstadt, Germany) and Sigma-Aldrich (Taufkirchen, Germany).

2.1.2 Kits

Amaxa® NHEM- Neo Nucleofector® Kit	Lonza (Köln, Germany)
Amaxa Cell line Nucleofector® Kit V	Lonza (Köln, Germany)
LightCycler® 480 FastStart DNA Master ^{PLUS} SYBR Green I Kit	Roche (Mannheim, Germany)
Apoptosis Detection Kit (APO- BRDU™)	BD Biosciences (Heidelberg, Germany)
DuoSet ELISA Development Kit	R&D Systems (Abingdon, UK)
Human Inflammatory Cytokines Multi-Analyte ELISA Array Kit	Qiagen (Hamburg, Germany)

2.1.3 Cell culture media and reagents

Cell culture media and reagents were purchased from BD Biosciences (Heidelberg, Germany), Gibco/Invitrogen (Carlsbad, USA), Promega (Mannheim, Germany) and Sigma-Aldrich (Taufkirchen, Germany).

Lipofectamine™ RNAiMAX Transfection Reagent	Invitrogen (Darmstadt, Germany)
Opti-MEM® I	Invitrogen (Darmstadt, Germany)
Penicillin Streptomycin (Pen/Strep)	Invitrogen (Darmstadt, Germany)
Trypsin-EDTA, 0.05% (1X)	Invitrogen (Darmstadt, Germany)
Cytostatics	Center for cytostatic preparation UKE(Hamburg, Germany)
InSolution™ ATM Kinase Inhibitor	Millipore (Bedford, USA)

2.1.4 Reagents for molecular biology methods

dNTPs[100mM]	PeqLab (Erlangen, Germany)
Random Primers [50 µg/mL]	Promega (Mannheim, Germany)
M-MLV Reverse Transcriptase [200 u/µL]	Promega (Mannheim, Germany)
M-MLV RT 5X Buffer	Promega (Mannheim, Germany)
RNasin® Plus RNase Inhibitor [40 u/µL]	Promega (Mannheim, Germany)
TRIzol Reagent	Invitrogen (Darmstadt, Germany)

2.1.5 Reagents for protein chemical methods

SeeBlue® Plus2 Prestained Standard (1X)	Invitrogen (Darmstadt, Germany)
RIPA Lysis Buffer (1X)	Santa Cruz (Heidelberg, Germany)
Amersham ECL™ Western Blotting Detection Reagents	GE Healthcare (Heidelberg, Germany)
Amersham Hyperfilm™ ECL	GE Healthcare (Heidelberg, Germany)
RNasin® Plus RNase Inhibitor [40 u/µL]	Promega (Mannheim, Germany)
PVDF Membrane Immobilion-P	Millipore (Bedford, USA)

2.1.6 Buffers

Lysis buffer

RIPA Lysis buffer 1X	1 mL
PMSF 200 mM	10 µL
Sodium orthovanadate 100 mM	10 µL
Protease Inhibitor Cocktail	10 µL

Loading buffer

50% Glycerol	10 mL
10% SDS	2 g
β-Mercaptoethanol	1 mL
1 M Tris pH 6.8	8 mL
Bromophenol	210 mg
ddH ₂ O	1 mL

MATERIALS AND METHODS

10X SDS running buffer

Tris	60.5 g
Glycine	288 g
10% SDS	200 mL
ddH ₂ O	ad. 2 L

50X CAPS

CAPS	111 g
NaOH	ad.pH 10.5
ddH ₂ O	ad. 1 L

Transfer buffer for Western blot

50X CAPS	40 mL
Methanol	400 mL
ddH ₂ O	ad. 2 L

10X TBS

1.5 M NaCl	87 g
0.5 M Tris	60.57 g
ddH ₂ O	ad. 1 L
pH 7.3 – 7.4	

1X TBST

10X TBS	100 mL
Tween-20	500 µL
ddH ₂ O	ad. 1 L

Stripping buffer

Glycine	15 g
SDS	1 g
Tween20	10 mL
ddH ₂ O	ad. 1 L
pH 2.2	

2.1.7 Oligonucleotides

2.1.7.1 Primers

Following primers (Metabion, Martinsried) were used for the analysis of the corresponding genes by means of qRT-PCR:

Primer	Sequence [5' → 3']
GAPDH ₁	fwd: GCA TCC TGG GCT ACA CTG A rev: CCA GCG TCA AAG GTG GAG
GAPDH ₂	fwd:CTCTGCTCCTCCTGTTTCGAC rev: ACGACCAAATCCGTTGACTG
GAPDHmouse	fwd: AGC TTG TCA TCA ACG GGA rev: TTT GAT GTT AGT GGG GTC
MITF ₁	fwd: AGT CAA CCG CTG AAG AGC AG rev: GGA GCT TAT CGG AGG CTT G
MITF ₂	fwd: TGC TAG AAT ATA ATC ACT ATC AGG TG rev: TGC TAA AGT GGT AGA AAG GTA CTG
MITFmouse	fwd: GAC ACC AGC CATA AAC GT rev:TTTT CCA GGT GGG TCT GC
XPG	fwd:CCA AGC GCA GAA GAA CAT TA rev: TTA AGC AAGCCT TTG AGT TGG
XPGmouse	fwd: GCG AAC ACT GTT TGA AGC AA rev: TCT TCA GCA AGC CTT TCA GC
p65	fwd: ACC GCT GCA TCC ACA GTT rev: GGA TGC GCT GAC TGA TAG C
NEMO	fwd: ACA TCA AGA GCA GCG TGG T rev: GCT GGA GCT GTT TGA G
ATM	fwd: ACT CCC AGC TTC TCA AGG ACA GT rev: TTA ATA CAT TCT CTT TGT GAG TTG TCCAT
Ikkβ	fwd: GGC ACG CTG GAC GAC CTA rev: CTC GAG GTT TTT CCC TTA GTC TC
IL8	fwd: AGGAAG AAA CCA CCG GAA GG rev: TGG CAA AAC TGC ACC TTC ACA CAG
IL1-α	fwd: GGT TGA GTT TAA GCC AAT CCA rev: TGC TGA CCT AGG CTT GAT GA

MATERIALS AND METHODS

Primer	Sequence [5' → 3']
TNF- α	fwd: CAG CCT CTT CTC CTT CCT GAT rev: GCC AGA GGG CTG ATT AGA GA

2.1.7.2 siRNA

siRNAs were purchased from Thermo Fisher Scientific (Leicestershire, United Kingdom).

siRNA	Sequence [5' → 3']
siScramble	GAA UGA CGA GAA GAU AUA A
siMITF	GAA CGA AGA AGA AGA UUU A

2.1.8 Antibodies

Anti-Microphthalmia mouse monoclonal AB	Millipore (Bedford, USA)
Anti- mouseMicrophthalmia goat polyclonal AB	Santa Cruz (Heidelberg, Germany)
Anti-MITF (C5) mouse monoclonal IgG ₁	Santa Cruz (Heidelberg, Germany)
Anti- XPG mouse monoclonal AB	Millipore (Bedford, USA)
Anti- XPG rabbit polyclonal AB	Sigma- Aldrich (Taufkirchen, Germany)
Anti- mouseXPG goat polyclonal AB	Santa Cruz (Heidelberg, Germany)
Anti- NF κ B p65 subunit rabbit monoclonal AB	Epitomics (Burlingame, USA)
Anti-p65 (Phospho S536) rabbit monoclonal AB	Abcam (Cambridge, UK)
Anti-p65 (phospho S536) rabbit polyclonal AB	Abcam (Cambridge, UK)
Anti-IKK γ mouse monoclonal AB	Millipore (Bedford, USA)
Anti-IKK γ (phospho S85) rabbit polyclonal AB	Abcam (Cambridge, UK)
Anti- β -Actin mouse monoclonal AB	Sigma- Aldrich (Taufkirchen, Germany)
Anti-Pt-(GpG) 'R-C18' rat monoclonal AB	Gift from Prof. Dr. Thomale
Anti-Thymine dimer (clone KTM53) mouse monoclonal AB	Kamiya Biomedical (Seattle, USA)
Anti-ATM rabbit monoclonal AB	Epitomics (Burlingame, USA)
Anti ATM phospho (pS1981) rabbit monoclonal AB	Epitomics (Burlingame, USA)
Anti-Ikk β rabbit polyclonal AB	Abcam (Cambridge, UK)

MATERIALS AND METHODS

Anti-Ikk β (phosphoY199) rabbit polyclonal AB	Abcam (Cambridge, UK)
FITC Goat Anti-mouse AB	Dako Cytomation (Hamburg, Germany)
Cy3 AffiniPure goat anti-rabbit IgG, F(ab') ₂ AB	Jackson ImmunoResearch (Suffolk,UK)
Alexa Fluor® 488 donkey anti-Mouse IgG (H+L) AB	Invitrogen (Darmstadt, Germany)
FITC goat anti-rat AB	Dianova (Hamburg, Germany)
Alexa Fluor® 488 rabbit anti-FITC AB	Invitrogen (Darmstadt, Germany)
Alexa Fluor® 488 goat anti-rabbit AB	Invitrogen (Darmstadt, Germany)
Polyclonal Goat anti-rabbit AB (IgG _{2a}) /HRP	Dako Cytomation (Hamburg, Germany)
Polyclonal Goat anti-mouse AB (IgG _{2a}) /HRP	Dako Cytomation (Hamburg, Germany)
2.1.9 Equipment	
Amaxa- Nucleofector II	Lonza (Köln, Germany)
Bioruptor UCD-200	Diagenode (Liège, Belgium)
CL-1000 Ultraviolet Crosslinker	UVP (Upland, USA)
UV Stratalinker 1800	Stratagene (La Jolla, USA)
ConfoCor 2 fluorescence microscope	Carl Zeiss Microscopy (Jena, Germany)
Light Cycler® 480	Roche (Mannheim, Germany)
NanoDrop 2000 Spectrophotometer	Thermo Scientific (Asheville, USA)
Thermocycler T3000	Biometra (Göttingen, Germany)
Flow Cytometer	BD FACS Canto with FACS Diva Software, Beckton Dickinson (Heidelberg, Germany)
Infinite®200	Tecan (Männerdorf, Switzerland)
ELx405™ Select Deep Well Microplate Washer	Biotek® (Bad Friedrichshall, Germany)

2.1.10 Plastic ware

Plastic ware for cell culture	Sarstedt (Nümbrecht, Germany)
Isopore™ membrane filters	Millipore (Bedford, USA)
ImmunoSelect adhesion slides	Squarix Biotechnology (Marl, Germany)
Microtiter 96-well plates	Maxisorp®, Nunc (Frankfurt, Germany)
PS-96-well microplates (U-Shape)	Greiner bio-one (Frickenhausen, Germany)

Additional used equipment and plastic ware not listed above correspond to current labor standard.

2.2 Methods

2.2.1 Cell biology methods

2.2.1.1 Cell culture

HumanA375, MALME3M and MeWo melanoma cells as well as murine B16V melanoma cells were obtained through ATCC and DSMZ (Braunschweig, Germany). HaCaT cells were kindly shared by Dr. Johanna Brandner (UKE, Hamburg). These cell lines were cultivated with DMEM supplemented with 10% FCS and 1% Penicillin/Streptomycin. The human 501mel cell line was a kind gift of Dr. Ruth Hallaban (Yale, New Haven) and the cell culture used for these melanoma cells was the F10 complemented with 10% FCS and 1% Pen/Strep. Primary human melanocytes were obtained from Yale Dermatology Cell Culture Facility (New Haven) cultivated in MCDB153 medium (Sigma-Aldrich) supplemented with 4% FCS, 1% penicillin/streptomycin, 5µg/ml insulin, 1 µg/ml transferrin, 0.6 ng/ml human basic FGF, 10ng/ml TPA and 13µg/ml BPE (bovine pituitary extract). Primary cells were studied after limited expansion at low passage numbers (n<11). Cells were grown in humidified incubators at 37°C supplemented with 5% CO₂.

2.2.1.2 UV exposure/ γ -irradiation

For UV-irradiation, cells were washed twice with PBS and, without lid, subsequently exposed to either 50 J/m² or 100 J/m² UVB at a wavelength of 302 nm in a CL-1000 Ultraviolet Crosslinker and to UVC at a wavelength of 254 nm in a Stratalinker 1800 at 100 J/m². Localized UV irradiation was carried out through pores of a

polycarbonate membrane measuring 3 μm in diameter. After irradiation, cells were grown in full medium until harvesting. Similarly, for γ -irradiation, cells were washed twice with PBS and filled up with medium. Exposure to 10Gy with covered plates followed, using a Cs-137 source.

2.2.1.3 Treatment with kinase inhibitors and cytostatics

Medium from cells assigned to kinase inhibitor assays was discarded and replaced with 1 μM ATM kinase inhibitor or DMSO 1hr before UVB irradiation and after UV exposure.

For cytostatic treatment, cell-medium was replaced with medium containing cisplatin (20 μM or 20 $\mu\text{g/ml}$), carboplatin (55 $\mu\text{g/ml}$), etoposide (10 $\mu\text{g/ml}$) or paclitaxel (50 nM). At different time points, cells were harvested and processed for diverse analyses.

2.2.1.4 Transfection with siRNA

For RNA interference, primary melanocytes and melanoma cells were transfected with 700 nM siRNA control or 2 μM siRNA MITF using the Amaxa NHEM-Neo Nucleofector Kit and the Amaxa Cell line Nucleofector Kit V, respectively. Briefly, 1×10^6 cells were pelleted and siRNA transfected using program U16 (I^omel cells) or A20 (melanoma cell lines) according to manufacturer's protocol and subsequently seeded with fresh medium in 6 cm-plates.

Alternatively, cells were seeded and 24 hr later transfected with 16 nM siScr or siMITF by the use of Lipofectamine RNAiMAX following the manufacturer's protocol. Cells were incubated with the transfection mix for at least 4 hr which was subsequently replaced by fresh medium.

2.2.2 Molecular biology methods

2.2.2.1 Apoptosis assay

Subsequent to transfection and cytostatic treatment or γ -irradiation of the murine melanoma cell line B16V cell, apoptosis was addressed by the recognition of 3' DNA fragments using the APO-BRDU™ kit as described by the manufacturer. Detection of fragmented DNA was assessed by FACS-based immunofluorescence.

2.2.2.2 Cell cycle analysis

Primary human melanocytes were transfected and irradiated with UVB. After harvesting and as a final step in the FACS-based DNA-damage-repair assay, cells were washed with PBS and resuspended in 0.05mg/ml PBS-propidium iodide. Samples were incubated in dark for 30min and analyzed by flow cytometry on a BD Canto machine. Standard deviations were calculated from biological triplicates and significance was demonstrated by a two-tailed t-test.

2.2.2.3 DNA damage repair analysis

Primary melanocytes, 501mel cells and B16V cells were transfected with either siMITF or siScr and subsequently analyzed for DNA lesions caused by either UV irradiation or cisplatin treatment by means of immunofluorescence.

2.2.2.3.1 UV- induced DNA lesions

In I^omel cells, CPDs were immunolabeled and measured by FACS. Briefly, cells were trypsinized at different time points after UVB irradiation (100 J/m²) and fixed in ice-cold 75% ethanol overnight at -20°C. After several wash steps with 2N HCl with 1% Triton-X-100, 0.1M Na₂B₄O₇ and PBS, cells were resuspended in 100 µg/ml RNase-PBS and incubated for one hour at 37°C. Subsequently, cells were incubated with 1:500 anti-thymine dimer or anti-streptavidin control antibodies for 1hr, washed and incubated with FITC-coupled goat anti-mouse secondary antibody (1:500) for 30 min protected from light. Finally, cells were washed and resuspended in PBS and fluorescence signals were measured by flow cytometry on BD FACS Aria or Canto II machines. Diva software (BD) was used for data acquisition and analysis. Standard deviations were calculated on the basis of the mean of biological triplicates. For statistical significance a two-tailed t-test was applied.

In 501mel cells, detection of immunolabeled CPDs was assessed by confocal microscopy and subsequently quantified using the ImageJ software. Signal intensity of more than 100 nuclei was measured and expressed in arbitrary fluorescent units (AFU).

2.2.2.3.2 Cisplatin- induced DNA lesions

Plated cells were treated with cisplatin (20 µg/ml) for 4 hr and were subsequently maintained in drug-free medium for up to 48 hr. At various time points, cell aliquots were harvested, washed in PBS, resuspended and placed on pre-coated microscopic slides. Subsequently, cells were fixed in methanol followed by alkaline denaturation

and sequential proteolytic digestion with pepsin (100 µg/ml) and proteinase K (100 µg/ml). After blocking with skim milk, Pt-(GpG) intrastrand cross-links in the nuclear DNA of single cells were immunolabeled with 0.1 mg/ml in PBS containing 1% casein and 200 mg of sonicated calf thymus DNA/ml and incubated for 2 hr at 37°C. After washing with 0.05% Tween 20 in PBS 2 min at 25°C, incubation with Cy3-rabbit anti-rat Ig secondary antibody followed. Nuclear DNA was detected by DAPI staining (200 µg/ml). Fluorescence signals from more than 100 individual nuclei were measured by ACAS 6.0 Cytometry Analysis System and expressed as arbitrary fluorescence units (AFU).

2.2.2.4 RNA isolation

For the RNA isolation of 5 to 10x10⁶ total cells 500 µl TRIZOL per 6-cm plate were added. Cells were scraped, transferred into a 1.5 ml tube and incubated with TRIZOL for 5-10 min at RT. Subsequently, 200µl chloroform were added, mixed and incubated for 2–3 min at RT. After centrifuging (15 min, 12000 g, 4°C) the aqueous RNA-containing phase (clear-, upper-layer) was transferred to a new tube and incubated for 10 min at RT with 1 volume isopropanol. Samples were centrifuged (10 min, 12000 g, 4 °C) and supernatant was discarded. Next, 1 ml Ethanol 75% was added to the pellet and vortexed following a centrifugation (5 min, 7500 g, 4°C). Finally, after discarding the supernatant, pellet was air-dried and subsequently resuspended in 50 µl RNase-free H₂O and incubated for 10min at 55-60°C.

Isolated RNA was quantified using a NanoDrop 2000 Spectrophotometer and either stored at -80 °C or further used.

2.2.2.5 cDNA synthesis

The conversion of whole RNA into cDNA was carried out by reverse transcriptase based on a two- step process, summarized below. For this purpose, 3 µg RNA were adjusted to a final volume of 28 µl with RNase-free water.

Step Nr. 1:

Mix:

Program:

Reagents	Volume X1 Sample	Temperature	Time
dNTPs	5 µl	70 °C	5 min
Random Primers	2 µl	4 °C	5 min
		4 °C	pause

Step Nr. 2:

Mix:

Program:

Reagents	Volume X1 Sample	Temperature	Time
M-MLV RT 5X buffer	10 μ l	37 °C	1 h
RNasin	1 μ l	95 °C	5 min
Reverse transcriptase	1 μ l	4 °C	pause

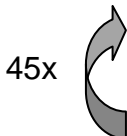
cDNA was stored at -20 °C or subsequently used for gene quantification by means of RT-PCR.

2.2.2.6 Real time PCR

This fluorescence-based method allows us to measure in Ct-values the transcriptional activity of a series of genes relative to an endogenous constitutive-expressing gene (*GAPDH*). For this purpose, LightCycler® 480 FastStart DNA Master^{PLUS}SYBR Green I Kit was used and reagents were mixed as follows:

Compound	Volume X1 Sample
H ₂ O _{dd}	4 μ L
Forward Primer [10 μ M]	1 μ L
Reverse Primer [10 μ M]	1 μ L
Master Plus	2 μ L

8 μ l Master Mix were pipetted in each of a 96-well plate followed by the addition of 2 μ l cDNA. For the negative control, cDNA was replaced by H₂O_{dd}. All samples were measured in triplicates, except the latter ones, which were assayed in duplicates. Importantly, due to the low RNA isolation rate in l^omel cells, 3 μ l of cDNA and H₂O_{dd} were used for the mix. Subsequently, 96-well plates were centrifuged (3 min, 900 r.p.m.) and measured in Light Cycler® 480. Following program was assessed:

	Step	Temperature	Time
	1	95 °C	10 min
45x 	2	95 °C	10 sec
	3	62 °C	10 sec
	4	72 °C	10 sec
	5	95 °C	1 sec
	6	65 °C	15 sec
	7	95 °C → 65 °C	gradient [0.11 °C/sec]
	8	40 °C	30 sec

Genes to be tested were called Genes Of Interest (GOI) and *GAPDH* was used as House Keeping Gene (HKG) in order to determine relative expression and fold induction (see formula 1 and 2, respectively):

Formula 1:

$$\text{Relative expression} = 2^{-(Ct(\text{GOI}) - Ct(\text{HKG}))} \times 1000$$

Formula 2:

$$\text{Fold induction} = 2^{-(\Delta Ct(t) - \Delta Ct(0h))} \times 1000$$

Depicted standard deviations were calculated from technical triplicates and significance was measured from biological triplicates using a two-tailed t-test.

2.2.3 Protein chemistry methods

2.2.3.1 SDS-PAGE (SDS-polyacrylamide gel electrophoresis) - WB (Western blot)

In order to address translational activity and phosphorylation status of determined proteins, treated cells were washed with cold PBS at different time points and subsequently scraped in 500 µl lysis buffer (Tris pH 6.8, 62.5 mM; SDS, 2.3%; glycerol, 10%; pyronin Y, 0.02% and β-Mercaptoethanol, 50 µl/ml). After transferring cell lysate into a new tube samples were incubated for 10min at 95°C. Lysates were centrifuged (10 min, 14000 r.p.m., 4°C) and resulting supernatants were stored at -80°C or immediately processed.

Alternatively, assayed cells were lysated by using 400 µl RIPA buffer. Samples were sonicated (5x à 30 sec sonification and 30 sec pause) followed by centrifugation for

MATERIALS AND METHODS

10 min, 10000 g at 4°C and supernatants were transferred into new tubes. Subsequently, quantification of whole protein was determined by means of Bradford analysis using NanoDrop 2000 Spectrophotometer. Depending on lysate availability, 25-40 µg protein lysates were mixed with 10 µl Loading buffer following an incubation of 10 min at 95°C. Samples were stored at –80°C or further used.

Next step was the separation of proteins according to their molecular weight under denaturing conditions by 10% or 8% resolving SDS-polyacrylamide gels. For 4 gels components were mixed as listed below.

Components	Running gel [mL]		Stacking gel [mL]
	8%	10%	5%
ddH ₂ O	9.3	7.9	2.7
30% acrylamide mix	5.3	6.7	0.67
1.5 M Tris pH 8.8	5	5	0.0
1.0 M Tris pH 6.8	0.0	0.0	0.5
10% SDS	0.2	0.2	0.04
10% ammonium persulfate	0.2	0.2	0.04
TEMED	0.012	0.008	0.004

Gels were subsequently loaded with samples and 15µl of SeeBlue® Plus2 Prestained Standard. Separation of proteins was performed at 24mA per gel for the first 15 min and at 30 mA for about 40 min in 10X SDS running buffer.

Transfer of separated proteins from gel to a PVDF (Polyvinylidene fluoride) membrane was carried out in a Wet blot system filled with CAPS buffer at 4°C for 4 hr at 500 mA or ON at 4°C at 90 mA with a final step of 4 hr at 500 mA.

Subsequently, membrane was shortly washed with 0.05% TBST buffer and incubated for 1hr in blocking buffer (5% non-fat dried milk powder in 0.05% TBST). Incubation with primary antibodies followed ON at 4°C (See table 1). Membrane was further washed twice for 5 min and once for 10min in 0.05% TBST followed by incubation with HRP-coupled secondary antibody (polyclonal goat anti-mouse antibody or polyclonal goat anti-rabbit antibody at 1:10000 or 1:5000 dilutions, respectively) for 1 hr at RT. Membrane was washed as described above. Proteins were finally detected

applying ECL solution on the membrane and capturing the signal on a film. Exposure times for the specific proteins varied from 10 sec to 15 min. Analysis of additional proteins was carried out first, by incubating the membrane twice with stripping buffer for 10min at RT followed by two-step washing in 0.05% TBST for 10 min and second, by repeating detection procedure from blocking of the membrane to ECL application.

Antibody	Dilution in 0.05% TBST
Anti- β -Actin	1:5000
Anti-MITF	1:1000
Anti-XPG	1:500
Anti-p65	1:1000
Anti-p65(phospho S536)	1:1000
Anti-IKK γ	1:1000
Anti-IKK γ (phospho S85)	1:1000
Anti-ATM	1:1000
Anti-ATM (phospho S1981)	1:1000
Anti-Ikk β	1:1000
Anti-Ikk β (phospho Y199)	1:1000

Table 1. Dilutions of primary antibodies for protein detection in WB

Experimental procedures assigned to WB analysis were reproduced at least three times.

2.2.3.2 Immunocytofluorescence (IF)

Phosphorylation and sublocalization of NEMO and p65 proteins were assessed by IF- based confocal microscopy. For this purpose, cells were seeded in 24-well plates on cover slips and transfected with 20 pmol siMITF or siScr, further following the protocol as described in 2.2.1.3 and with a subsequent UVB treatment. At different time points, cells were washed twice with cold PBS and fixed in ice-cold methanol for several hours. Cover slips were washed with washing buffer (WB; 0.5% BSA, 0.05% tween 20 in PBS) and subsequently blocked in blocking buffer (1% BSA in PBS) at RT. One hour later, cells were incubated with a mixture of primary antibodies (anti-MITF and -pS536 p65 antibodies or anti-MITF and -p86 NEMO antibodies) diluted 1:300 in WB for 1 hr at RT in a moist chamber. After a two-step washing with WB, a

mixture of secondary antibodies was applied in a 1:500 dilution in WB (45 min, RT in a moist chamber). After washing twice with WB and once with PBS, incubation of cover slips with DRAQ5™ (1:1000 in PBS, 5min, RT) followed for counterstaining of the nuclei. Ultimately, cover slips were mounted with polyvinyl alcohol mounting medium on slides. Fluorescence signals of more than 100 nuclei per sample were analyzed by ConfoCor 2 fluorescence microscope and measured by ImageJ Software. Statistical significance was determined by a two-tailed Mann Whitney test with a confidence interval of +/-95%.

2.2.3.3 ELISA (Enzyme Linked Immunosorbent Assay)

To address the potential MITF-dependency on the secretion of inflammatory cytokines, sandwich ELISA was applied. As previously described, cells were transfected with siRNA by means of Lipofectamine™ RNAiMAX Transfection system and subsequently UVB irradiated (50 J/m²). At several time points (24-, 48- and 72 hr post irradiation) supernatants were collected and analyzed using the DuoSet ELISA Development Kit following manufacturer's instructions with some variances. Briefly, microtiter plates were coated ON at 4°C with capture antibodies: 4 ng/ml (anti-TNF- α or -IL8 antibodies) or 2 ng/ml (anti-IL1- α or -IL10 antibodies). After washing with TBS, wells were blocked with blocking reagent for 1 hr at RT. Afterwards, a three-time washing step with TBS-T followed and subsequently 60 μ l of supernatants were added and incubated for at least 2 hr. Wells were washed three times with TBST following an incubation for 1hr with detection antibody: 0.15 ng/ μ l for IL10 AB, 0.05 ng/ μ l for IL1- α and TNF- α ABs and 0.02 ng/ μ l for IL8 AB. Eight-time washing with TBST was followed by incubation with horseradish peroxidase-coupled streptavidin (1:200) for 25 min. Finally, 100 μ l TMB substrate per well were applied and incubated until desired color intensity was achieved. Signals were detected at 455-575 nm by Infinite®200 and protein expression was quantified according to internal standards based on recombinant protein. Cell culture medium was used as negative control. Samples were assayed in technical duplicates. Standard deviations correspond to the mean of biological triplicates and significance was measured using a two-tailed t-test.

3 Results

3.1 MITF is involved in the repair of DNA lesions induced by UV irradiation and cisplatin treatment

To assess the hypothesized role of MITF in the DNA damage response under genotoxic attack, melanoma cell lines and primary melanocytes were UV irradiated or treated with cisplatin. MITF was depleted by RNA interference to study its impact on DNA repair. To this end, we carried out FACS and immunofluorescence analyses of CPD lesions upon siRNA mediated MITF repression vs. siRNA controls.

As shown in Figure 8A, in primary human melanocytes, UVB irradiation led to an induction of CPD-lesions with a maximum peak induction 2 hr post-irradiation. Early repair of CPD lesions is significantly hampered upon MITF depletion, potentially indicating an effect on transcription coupled repair, which occurs up to 11 hr after genotoxic attack [110-111]. From this time point forward, the CPD-signal decreased up to 24 hr upon UV exposure. Additionally, concomitant cell cycle analysis demonstrated a prolonged growth arrest in MITF depleted primary melanocytes accumulating in the G2/M phase and a reduction in presumptive translesion DNA replication (S-phase) 24 hr after UV irradiation (Figure 8B).

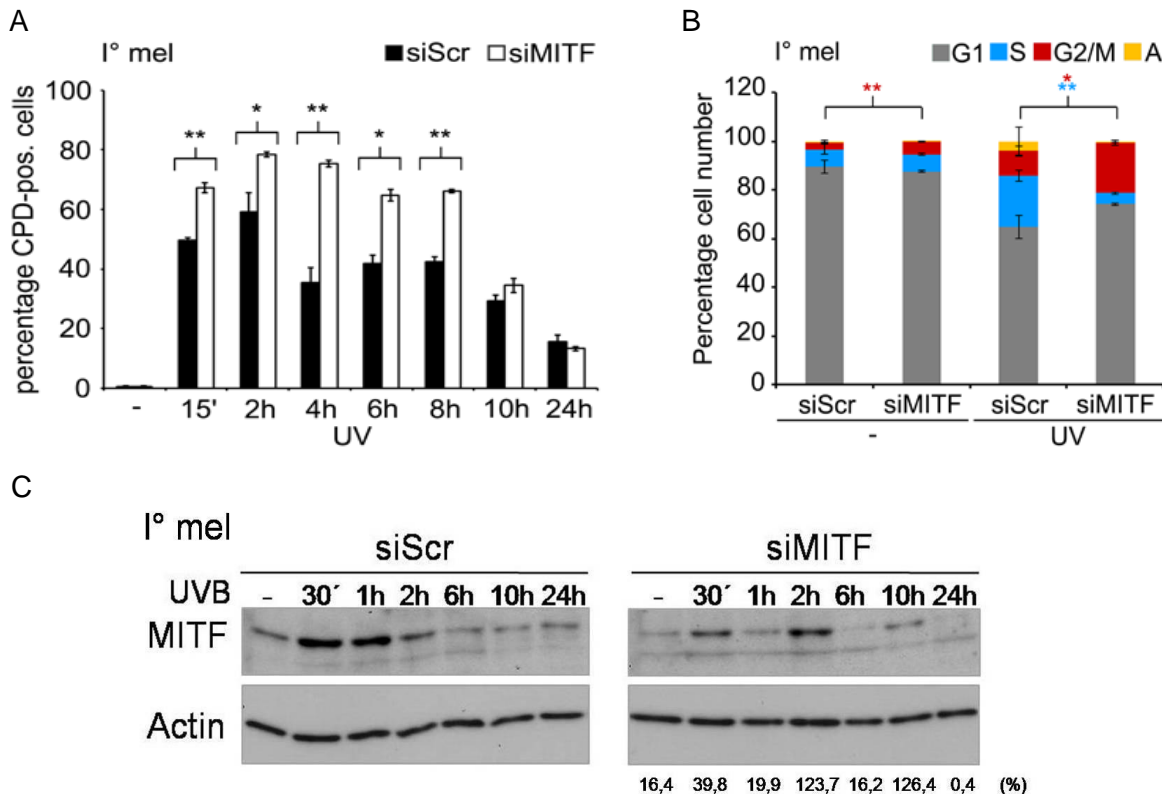


Figure 8. MITF regulates DNA damage repair capacity in UV irradiated primary melanocytes. Repair kinetics of CPD lesions over time in primary human melanocytes (A), which were transfected with either siMITF or siScr RNA and subsequently irradiated using UVB, 100 J/m². CPD were analysed

RESULTS

by flow-cytometry using an anti-CPD antibody. Results are expressed as the mean of the experiment done in triplicate \pm SD, two-tailed Student's test; * $p < 0.05$; ** $p < 0.01$. (B) Primary melanocyte populations from (A) underwent FACS based cell cycle analyses. Relative distribution of cells in defined cell cycle phases under MITF knock down (siMITF) versus scrambled control (siScr) before (-) and 24 hr after UVR (UV) is given including error bars representing SD measured in biological triplicates (two-tailed Student's test; red, G2/M phase, * $p < 0.05$; ** $p < 0.01$; blue, S-phase, ** $p < 0.01$). (C) MITF knock down efficiency was analyzed by Western blotting. Actin served as loading control. Values beyond siMITF panel correspond to the percentage of MITF relative expression in MITF-depleted cells with regard to siScr-transfected cells.

In order to evaluate the NER regulation by MITF in a lesion-specific manner, cellular repair capacity of primary human melanocytes and B16V melanoma cells treated with cisplatin was tested. Cisplatin is a DNA damaging drug leading to Pt(GpG) intrastrand adducts, which induce NER, as well as intra- and interstrand crosslinks. A microscopy-based fluorescence assay of immunolabeled Pt(GpG) intrastrand adducts in both siScr or siMITF transfected primary human melanocytes and B16V murine melanoma cells was applied. In analogy to UVR-induced DNA lesions, repression of MITF entailed significantly delayed repair kinetics of Pt-(GpG) intrastrand DNA adducts in primary melanocytes (Figures 9A and B) and melanoma cells (Figures 10A and B) after a transient exposure to cisplatin. In contrast to I^omel, MITF-depleted B16V cells exhibited a rebounding effect reaching the same Pt(GpG) levels as those of control cells 48 hr after cisplatin treatment.

RESULTS

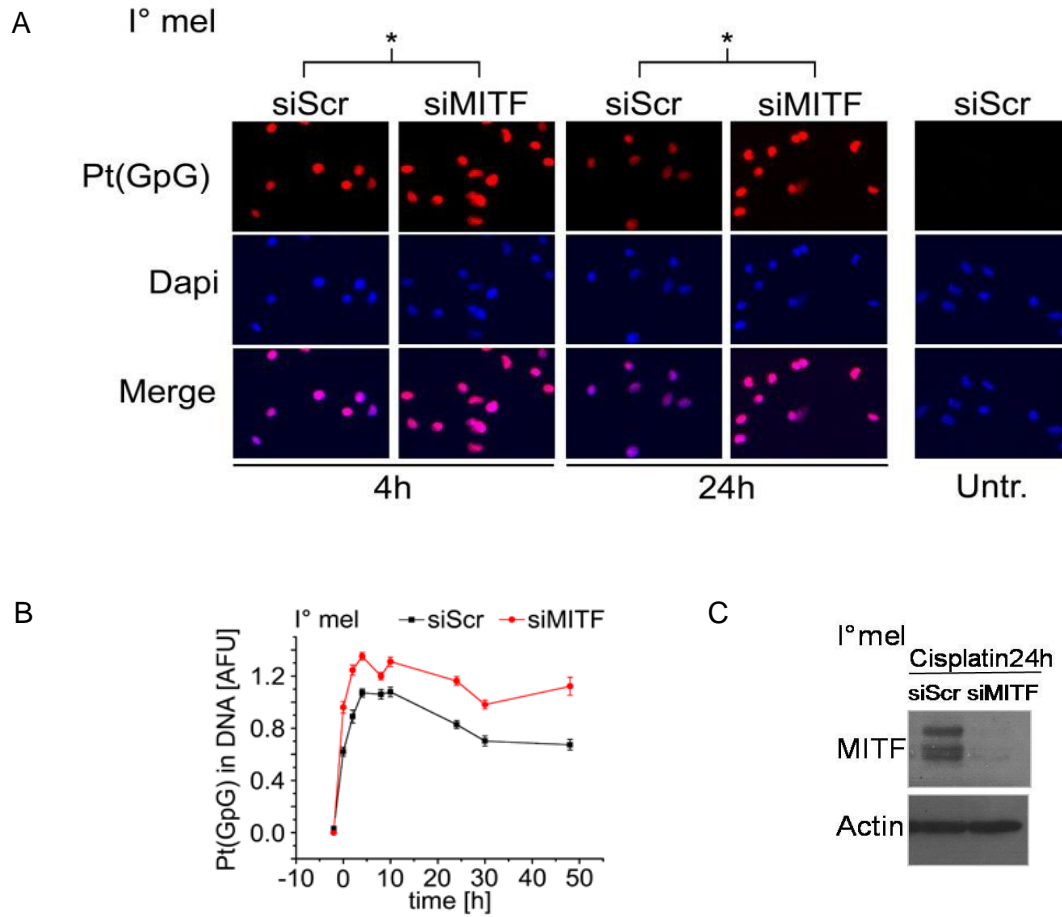


Figure 9. Detection of cisplatin-induced Pt-(GpG) intrastrand adducts in nuclear DNA of I°mel cells after cisplatin exposure. IF microscopy using an antibody directed against cisplatin-induced Pt-(GpG) intrastrand adducts in nuclear DNA of I° melanocytes transfected with siScr or siMITF (A). Cell aliquots were analyzed for DNA adducts levels by *in situ* staining with R-C18 antibody (red). DNA was counterstained with DAPI (blue). (B) Repair kinetics of cisplatin-exposed cells was quantified by ICA analysis. AFU values represent means of >100 cell nuclei +/- 95% CI (*). Scale: 10 μ m. (C) shows MITF knockdown efficiency assessed by Western blot. Actin served as loading control. (A, B in collaboration with Jürgen Thomale, University Essen).

RESULTS

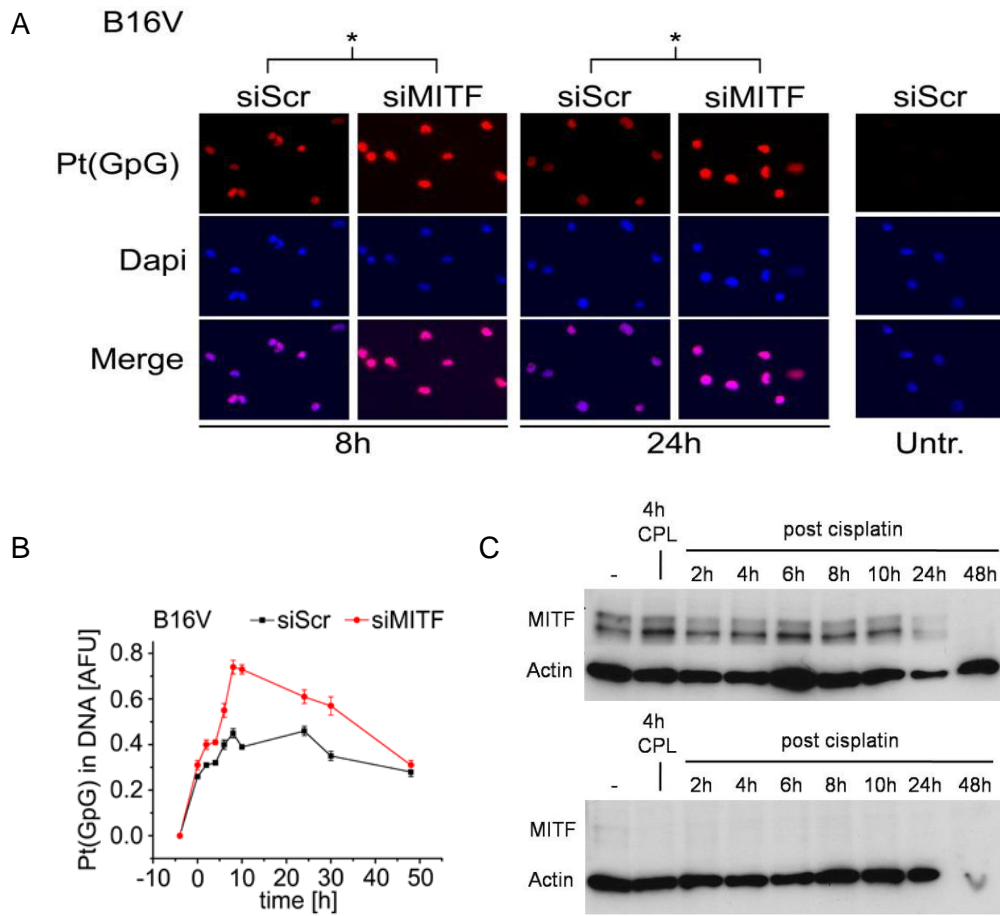


Figure 10. DNA damage repair capacity is regulated by MITF in B16 V murine melanoma cells upon cisplatin exposure. B16 V cells were siScr- or siMITF- transfected and subsequently transiently treated with cisplatin (20 μ g/ml). (A) Pt-(GpG) intrastrand adducts (red) were analyzed by immunofluorescence microscopy (blue: DAPI [DNA]). DNA adducts repair kinetics were quantified by ICA analysis (B). AFU values represent means of >100 cell nuclei \pm 95% CI (*). Scale: 10 μ m. MITF knockdown efficiency is depicted in (C). Upper panel and lower panel correspond to siScr- and siMITF transfected cells, respectively. Equal loading control was determined by actin signal.

3.2 MITF's role in DNA damage repair under UVB irradiation is partially mediated through the regulation of XPG

Our group succeeded in showing a close relationship between MITF and the cellular response to UV exposure, demonstrating a transcriptional and translational up-regulation of MITF under UVB irradiation. In I° melanocytes MITF protein showed an oscillatory activation peaking at 30 min and 10 hr post-irradiation and a migratory shift to a slower mobility form corresponding to a phosphorylated, transactivating form [73] (Figure 11).

The results shown above involving MITF in the nucleotide excision repair system and previously published data [61] suggested that the endonuclease XPG might be regulated by MITF in DNA damage response pathways. To assess this issue, qRT-PCR and Western blot analyses were applied to primary human melanocytes upon UV treatment. At both transcriptional and translational levels, XPG showed a similar oscillatory expression profile as that observed for MITF (Figure 11 and data not shown), demonstrating a marked induction of XPG protein 30min and 24hr after irradiation.

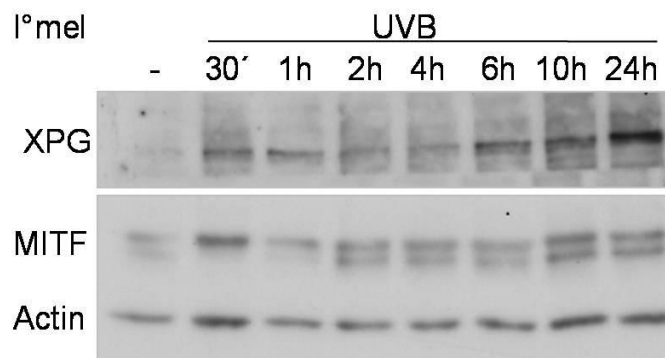


Figure 11. MITF and XPG induction under UV treatment in primary human melanocytes. Primary human melanocytes (I°mel) were UV irradiated using 50 J/m². MITF and XPG proteins from whole cell lysates were evaluated by immunoblot. Actin served as protein loading control

In order to elucidate whether this phenomenon was exclusively encountered in primary human melanocytes or preserved upon transformation into melanoma, a genetically heterogeneous panel of human melanoma cell lines was tested on MITF and XPG responsiveness to UVR that is presented in Table 2.

RESULTS

Melanoma cell lines	BRAF V599E	PTEN	N-ras	CDK4	CDKN2A (p16)	Ink4a/Arf (p16/p19)	p53	MITF Copies
A375	Mut	WT	WT	n.d	n.d	n.d	WT	2
Mewo	WT	n.d	WT	n.d	n.d	n.d	WT/Mut #	2
Malme 3M	Mut	n.d	n.d	n.d	HD	n.d	n.d	6
501 mel	WT	n.d	Mut	n.d	n.d	n.d	n.d	2
B16V*	WT	WT	WT	n.d	n.d	Del	WT	2

Mut = mutation

HD = homozygous deletion

* = If derivate from B16F

n.d. = no data

= controversial data

Del = deletion

Table 2. Molecular heterogeneity in melanoma cell lines. Depiction of some molecular features in selected melanoma cell lines.

Additionally, a keratinocyte cell line (HaCaT) was chosen which lacks M-MITF expression. Except for HaCaT cells, all melanoma cell lines were transfected with siRNA targeted against MITF or scrambled siRNA. 18 hr after transfection, cells were submitted to UVR. In those cell lines, in which MITF exhibited an endogenous and UV- inducible expression, *XPG* mRNA was induced with a maximum peak expression 9 hr post—UVR. In analogy to primary human melanocytes the transcriptional upregulation of *XPG* was abrogated by MITF knockdown. Interestingly, A375 melanoma cells, which lack endogenous MITF expression, did not show an induction of *XPG* after UV treatment. Similarly, HaCaT cells did not reveal a UV-induced upregulation of *XPG* (Figure 12).

The observed MITF dependent regulation of *XPG* transcripts was corroborated at the protein level in NER proficient human 501mel cells, which exhibit a constitutively high MITF protein expression. RNA interference mediated MITF depletion resulted in abrogation of *XPG* induction upon UVB treatment (Fig 13A).

Additionally, a microscopy-based fluorescence assay was applied in locally UV irradiated 501mel cells revealing a significant reduction in NER efficiency and nuclear *XPG* assembly 10 hr post-irradiation under MITF knockdown conditions (Figure 13B), recapitulating results obtained by Western blotting.

RESULTS

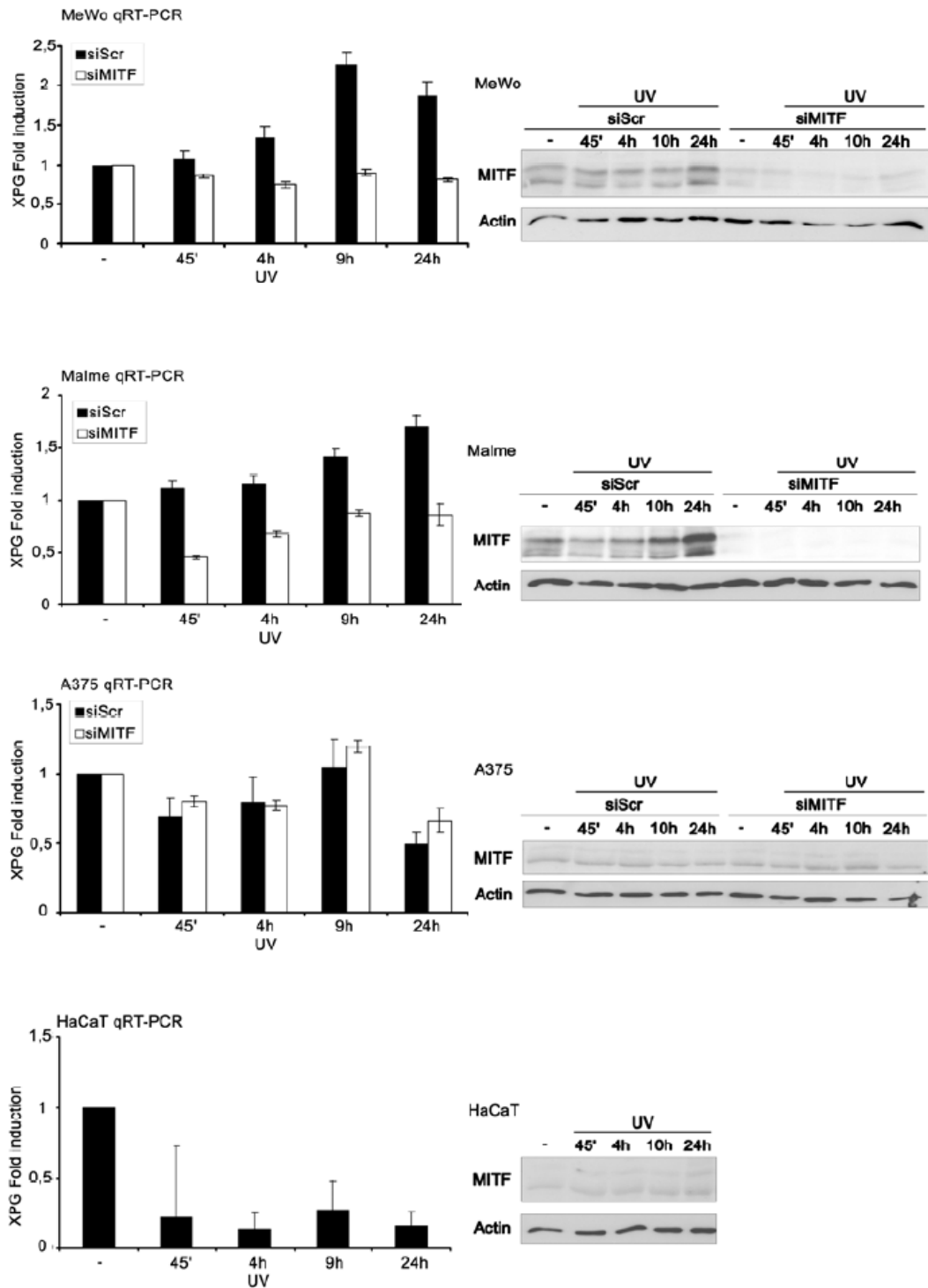


Figure 12. Regulation of MITF and *XPG* after UV irradiation in different cell lines. Cell lines were irradiated with UVB (50 J/m²) after transfection with siRNA against MITF or siScr. *XPG* transcripts were analyzed by means of quantitative RT-PCR. *XPG* expression was normalized to *GAPDH* and calculated as fold-induction compared to baseline. Immunoblot analyses show UV responsiveness of MITF protein and efficiency of the knockdown. Actin is used as loading control. Error bars show the standard deviations from the mean, measured in technical triplicates.

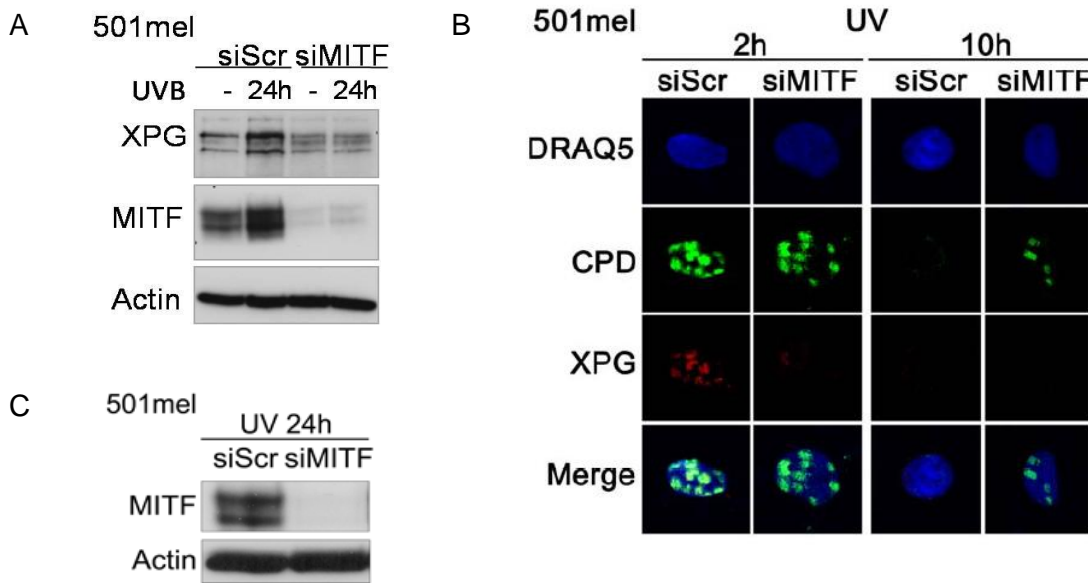


Figure 13. Regulation of MITF and XPG after UV irradiation in 501mel cells. (A) 501mel cells were transfected with siMITF or siScr and subsequently treated (24hr) or not (-) with 50 J/m² UVB. MITF and XPG protein profile was examined by immunoblot analysis. Equal loading was validated by actin. (B) Repair kinetics of CPD lesions over time in 501mel cells, which were transfected with either siMITF or siScr RNA and subsequently irradiated with UVC (200 J/m²) using a polycarbonate membrane with 3 μm pores. Recruitment of XPG (red) protein to sites of UV damage and CPD (green) immunolabelling are shown by confocal microscopy. Nuclear DNA was counterstained with DRAQ5 (blue). (C) MITF knockdown efficiency in 501mel cells was validated by Western blotting using actin as loading control. (B) and (C) are courtesy of Dr. M. Seoane Souto.

3.3 The regulation of XPG by MITF is DNA lesion specific

To test whether the transactivation of XPG by MITF is dependent on the genotoxic context, murine B16V melanoma cells were submitted to a diversity of cytotoxic treatments implying different DNA damage repair mechanisms. To define the appropriate experimental conditions FACS-based apoptosis studies were undertaken under genotoxic stress (data not shown). In B16V cells, continuous cisplatin exposure led to a marked oscillatory upregulation of MITF and XPG with maximum activation at 30 min and 24hr post-treatment (Figure 14A). However in contrast to UVR, cisplatin treatment resulted in a transcriptional activation of XPG independent of MITF (data not shown).

Likewise, carboplatin, a drug belonging to the platinum family, induced an upregulation of both *MITF* and *XPG* transcripts the latter of which was independent of MITF as shown by MITF directed RNA interference (Figure 14B).

RESULTS

By contrast, paclitaxel, a microtubule-stabilizing reagent, and etoposide, a DNA strand breaking topoisomerase II inhibitor, caused an activation of MITF, but XPG did not exhibit any response (Figure 14C and D, respectively).

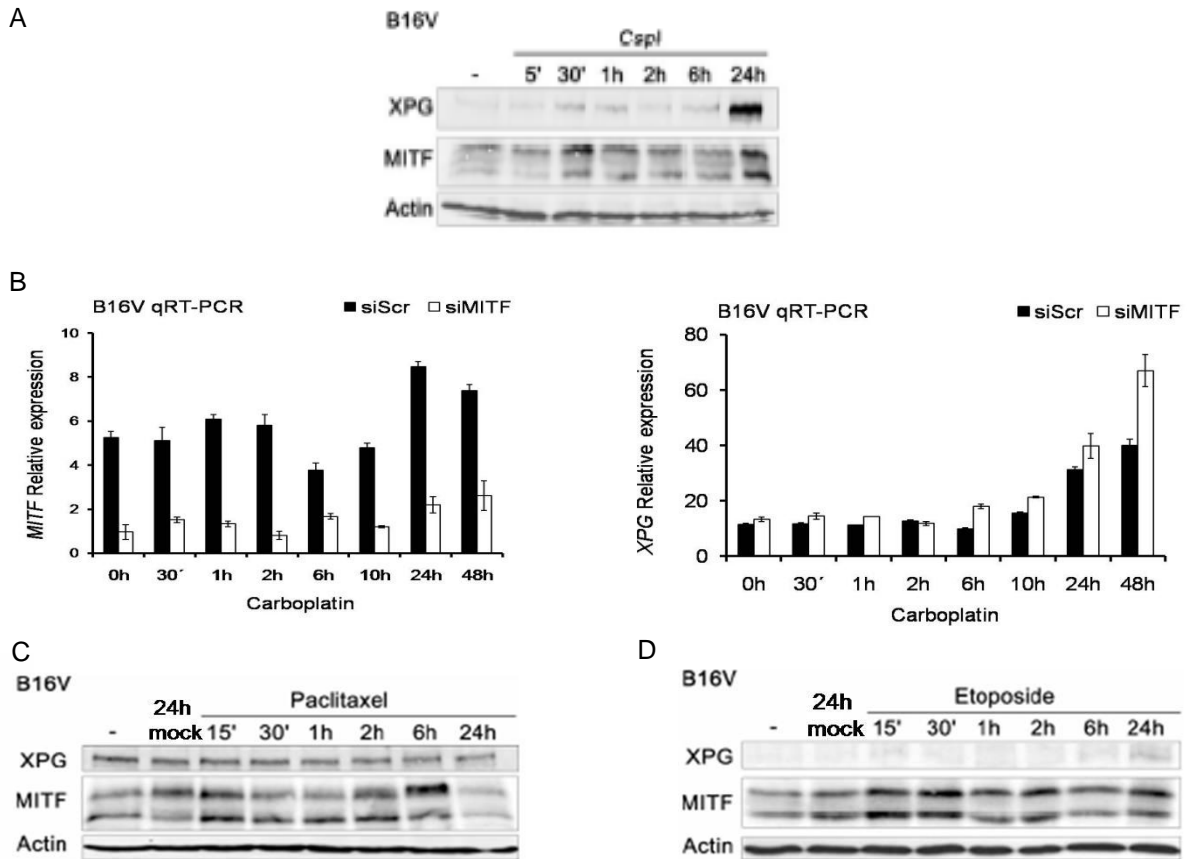


Figure 14. MITF mediated upregulation of XPG is dependent on the genotoxic context. Murine melanoma cells B16V were treated with cisplatin (20 μ M), paclitaxel (50 nM) or etoposide (10 μ g/ml) for different time points (A, C and D, respectively). Whole cell lysates were immunoblotted for mouse XPG and mouse MITF. Actin was used as loading control. (B) B16V cells were transfected with siMITF or siScr and treated with carboplatin (55 μ g/ml) and harvested at different time points. Modulation of MITF and XPG mRNA expression was analysed by quantitative RT-PCR and is represented as relative expression and fold induction, respectively. Values depicted in the qRT-PCR analysis are presented as mean \pm SD measured in technical triplicates of one out of three independent experiments. (A) is a courtesy of Dr. K. Kaufmann.

In B16V cells, γ -irradiation also resulted in an oscillatory expression profile of MITF protein with peak induction at 30 min and 24hr after treatment (Figure 15 A). Since the immunoblot analysis did not yield conclusive data on XPG responsiveness upon γ -irradiation we applied real-time PCR that showed a transcriptional induction of

RESULTS

XPG, as well as *MITF*, both of which reached a delayed maximum level at 72 hr post-irradiation. However, the upregulation of *XPG* was independent of MITF, as *XPG* transcriptional activity was not abrogated under MITF knockdown conditions (Figure 15B).

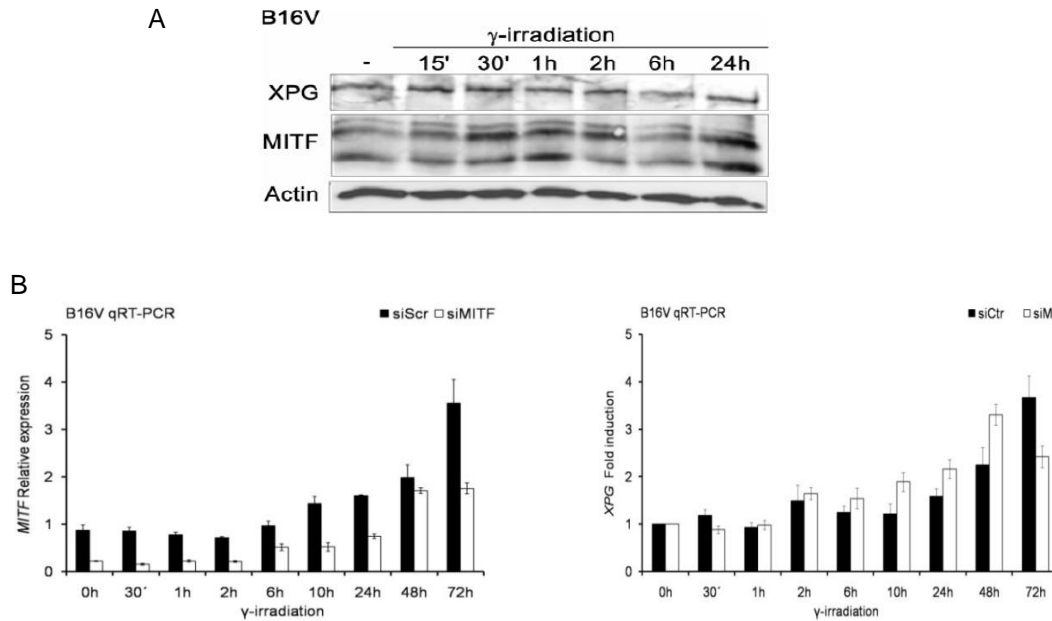


Figure 15. XPG upregulation is not dependent on MITF expression under γ -irradiation. siScr or siMITF-transfected murine B16V cells were treated with γ -irradiation (10Gy) and harvested for different time points. Whole cell lysates were analyzed for XPG and MITF by immunoblotting (A) and qRT-PCR (B). Actin was used as loading control. *MITF* and *XPG* transcripts are presented as relative expression and fold induction, respectively. Error bars show the standard deviations from the mean, in technical triplicates. Data shown here are representative of three experiments.

3.4 The role of MITF in the DNA damage response under UVB exposure is also mediated by the regulation of ATM

Given MITF's role in nucleotide excision repair as a functional endpoint of a DNA damage response, we asked whether MITF is also involved in inflammatory reaction pathways both of which are induced by UVR.

Previous data suggested a regulatory effect of MITF on the ATM kinase, which is a key sensor of DSB but also activated upon UVR [96, 112]. Since ATM had been identified as a direct transcriptional target of MITF, we first set out to assess ATM transcripts in the presence vs. depletion of MITF upon UVR of primary human melanocytes and 501melanoma cells. qRT-PCR analyses demonstrated a weak MITF-independent induction of *ATM* transcripts in I^o melanocytes visible at the 10 hr and 24 hr time points after UVB exposure, whereas 501mel cells exhibited a marked

RESULTS

oscillatory regulation with maximum induction 1 hr and 24 hr post-irradiation which was weakly abrogated upon MITF depletion (Figure 16B).

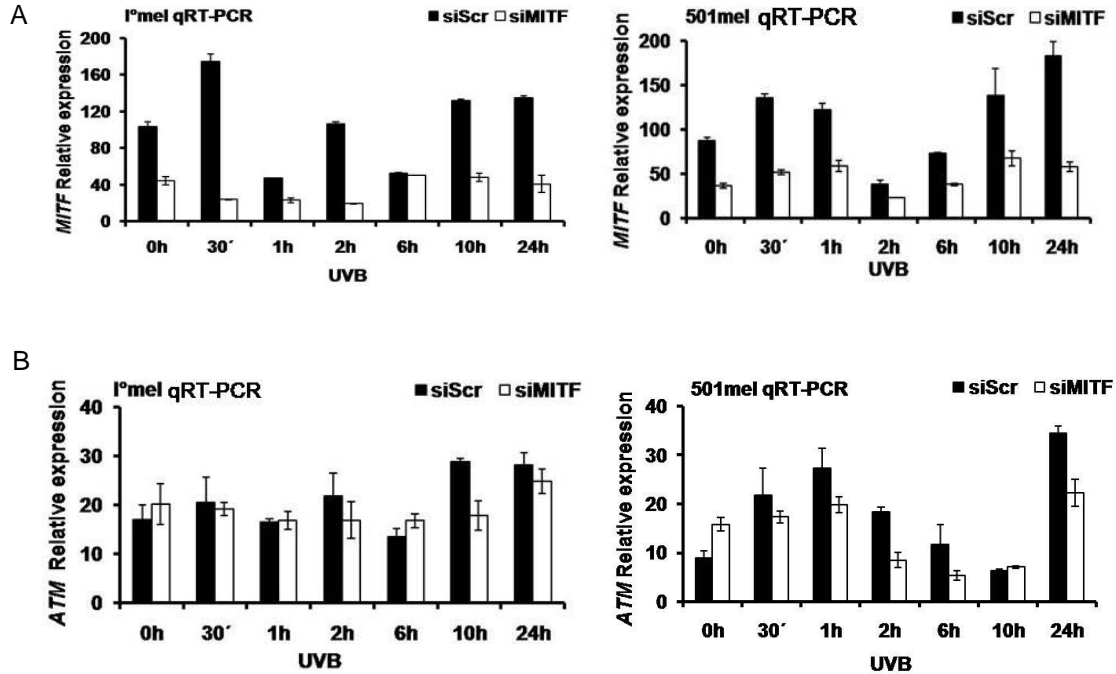


Figure 16. ATM transcriptional regulation by MITF under UVR in I°mel and 501mel cells. I°mel cells (left panel) and 501mel cells (right panel) were transfected with siRNA against MITF or siScr and subsequently irradiated with UVB (50 J/m²). MITF and ATM transcript levels (A and B, respectively) were analyzed as relative expression by means of qRT-PCR. Error bars show the standard deviations from the mean measured in technical triplicates. Data shown above are representative of three independent experiments.

The next step was to assess a possible regulation of ATM at the protein level. As mentioned above, ATM is regulated by posttranslational modifications which critically determine its functional state in the cell. In primary human melanocytes, ATM expression was induced 10hr and 24hr after UVB irradiation (considering a lower protein loading in the non UV-treated cells). This effect was abrogated under partial MITF repression (Figure 17 A left panel). In analogy, phospho-ATM signal increased upon UV treatment and was abrogated in siMITF-transfected cells (Figure 17B left panel).

Interestingly, in 501mel cells, ATM protein exhibited a weak responsiveness 24 hr after UVB irradiation. Under MITF knockdown conditions (Figure 17A), the basal expression and induction of ATM post- UVR was markedly reduced. MITF repression

RESULTS

resulted in an almost complete loss of the phospho-ATM signal, presumably due to the substantial decrease of the translational activity (Figure 17B right panel).

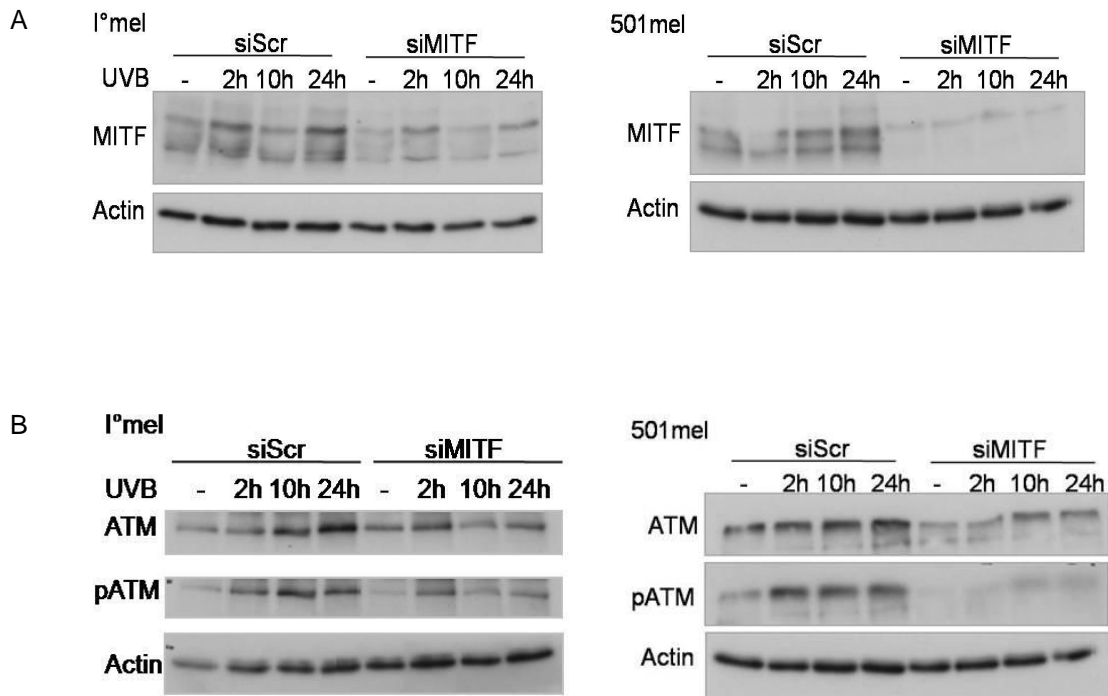


Figure 17. Analysis of ATM protein expression and p-(Ser1981) ATM after UVB treatment in I°mel and 501mel cells. I°mel cells (left panel) and 501mel cells (right panel) underwent UVR (50 J/m²) after transfection with siMITF or siScr and harvested at different time points. Whole protein lysates were tested for expression and phosphorylation of MITF and ATM by immunoblot (A and B, respectively). Equal loading was determined by detection of actin. pATM, phospho-ATM (Ser 1981).

3.5 In UV irradiated melanoma cells phosphorylation of Ser85- NEMO is mediated by ATM

ATM is a well-known activator of the NFκB canonical pathway in a genotoxic context. As mentioned above, this regulation is mediated by the phosphorylation of the master regulator of NFκB, NEMO. Hence, we tested whether the MITF-dependent regulation of ATM (phospho-) protein has an impact on NEMO expression and/or the activation of its phosphorylation at Ser85 under UV- irradiation.

For this purpose, 501mel cells were submitted to UVR (50 J/m²) after treatment with a specific ATM inhibitor or DMSO as a control, and whole cell lysates were immunoblotted for the detection of NEMO protein including its phosphorylated form (pSer85). As shown in Figure 18, pharmacological inhibition of ATM results in a marked reduction of NEMO phosphoactivity, albeit residual ATM phosphorylation is

RESULTS

visible in the presence of the inhibitor under UVB exposure. As anticipated the UV-mediated up-regulation of ATM protein is not affected by inhibition of its kinase activity. In contrast to ATM, NEMO protein abundance remains constant upon UVB exposure.

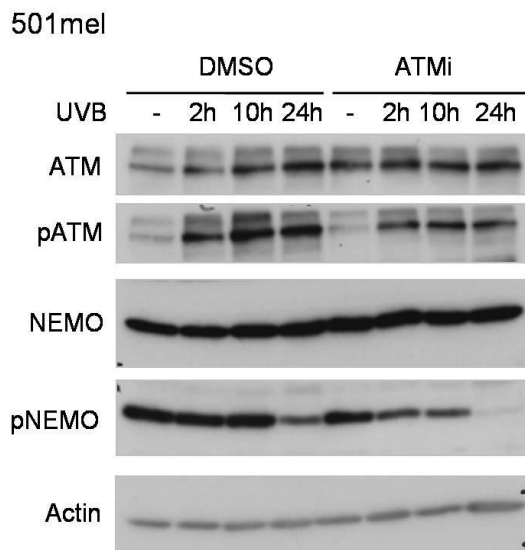


Figure 18. Phosphorylation of (Ser85) NEMO under UVB irradiation is dependent on ATM activation in 501mel cells. 501mel cells underwent UVR (50 J/m²) or not (-) after treatment with DMSO or ATM inhibitor. Western blot of whole protein lysates was applied to analyze the expression and phospho- status of ATM (Ser 1981) and NEMO (Ser 85). Actin served as loading control.

3.6 MITF regulates the NFκB pathway by transactivation of ATM

As outlined above, the NFκB pathway is activated under genotoxic conditions and plays an important role in DDR pathways. Given MITF's impact on ATM activity and the link between ATM and NFκB signaling, we set out to investigate a potential interplay between MITF and the NFκB pathway.

3.6.1 Transcriptional transactivation of NFκB is not dependent on MITF

Beside a transcriptional regulation of the DNA damage sensor ATM, MITF could potentially be involved in the transcriptional transactivation of the canonical NFκB pathway's downstream components. To address this hypothesis, we analyzed the mRNA expression of NEMO, IKKβ and p65 by means of qRT-PCR upon siRNA mediated repression of MITF vs. scrambled siRNA control.

In I^omel and 501 melanoma cells, NEMO transcripts reveal no modulation upon UVR regardless of MITF (Figure 19A, left panel). Similarly to NEMO, expression of IKKβ

RESULTS

and p65 transcripts was independent of MITF, albeit they did reveal a subtle oscillatory induction upon UVB exposure (Figure 19C, left panel).

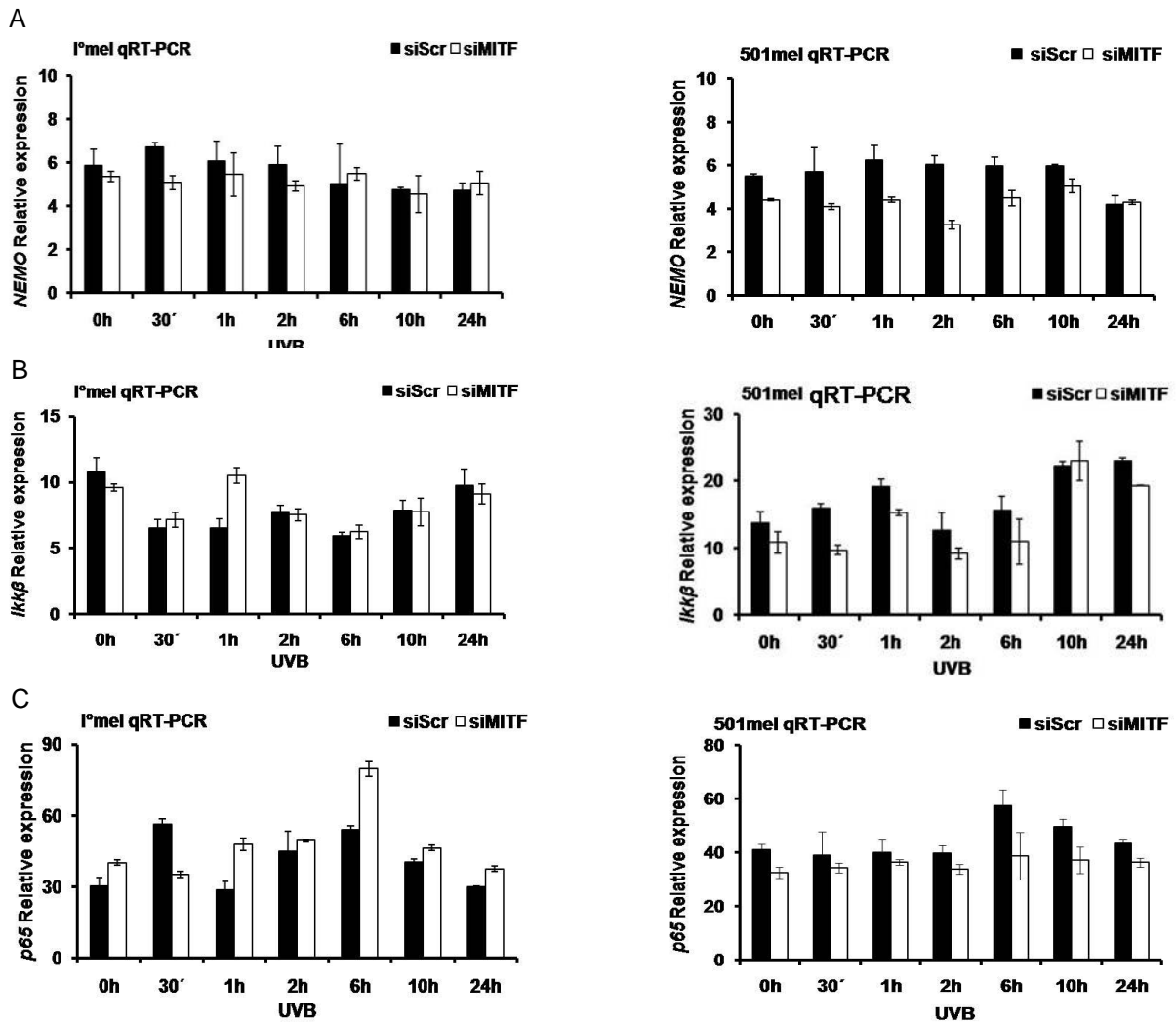


Figure 19. In primary human melanocytes and 501mel cells expression of *NEMO*, *IKKβ* and *p65* is not MITF-dependent under UVB treatment. I°mel cells (left panel) and 501mel cells (right panel) were UVB irradiated (50 J/m²) after transfection with siMITF or siScr. To assess relative expression of *NEMO*, *IKKβ* and *p65* (A, B and C, respectively) qRT-PCR was applied. Error bars show the standard deviations from the mean in technical triplicates. Depicted results are representative of three experiments.

3.6.2 MITF is involved in the activation of NEMO and p65 proteins under UVR

Complementary to the transcript analysis we subsequently evaluated the expression of NEMO, IKK β and p65 at the protein level by means of Western blotting.

Primary human melanocytes and 501mel cells show an analogous expression pattern for NEMO protein (Figure 20A left and right panel, respectively). In both cell types, NEMO translation is not affected by UVR and MITF depletion, recapitulating the results obtained by qRT-PCR.

In analogy to NEMO, immunoblot analysis of primary melanocytes and 501mel cells did not reveal a clear regulation of p65 protein expression upon UVR, nor did it show any MITF dependence (Figure 20B). At the posttranslational level, primary melanocytes lacked detectable phospho-activity of NEMO (Figure 20A left panel), whereas a marked but transient increase of Ser85 phosphorylated NEMO is discernible upon UVB exposure in 501mel cells. Under MITF knockdown conditions, this induction was also observed nevertheless in a reduced manner, arousing the suggestion of MITF's role in NEMO's phosphorylation under the aforementioned genotoxic exposure (Figure 20A right panel).

Analysis of phospho-Ser536 p65 in primary human melanocytes suggests responsiveness under UVR with an induction peak at 24 hr after UV exposure. Under MITF depletion, the maximum induction of phosphoactivity of p65 at 24 hr is clearly visible, however it appears to be reduced when compared with the corresponding time point under siScr transfection. (Figure 20B left panel). In 501mel cells, p65 phosphorylation is markedly reduced under MITF knockdown conditions at baseline and after UV treatment (Figure 20B right panel). These results indicate that the phosphorylation of p65 is dependent on MITF activity.

With regard to NEMO, the immunoblot analyses did not show conclusively that MITF has an impact on its activity since phospho-NEMO could not be detected in primary melanocytes and MITF-dependent differences in phosphoactivity in 501mel cells were confined to a single 10 hr time point (Figure 20A). On the other hand, the assessment of Ser-536 p65 in 501mel cells suggests a regulation of phosphorylation by MITF which cannot fully be explained by varying amounts of p65 protein. In primary melanocytes, maximum induction of p65 phosphoactivity is reduced under conditions of MITF depletion. In addition, phosphoactivity of p65 in 501mel cells appears to be reduced over the complete time course upon MITF depletion.

RESULTS

Intriguingly, we were not able to demonstrate a clear co-regulation of phospho-NEMO and p65 as anticipated in the NF κ B reaction pathway [112].

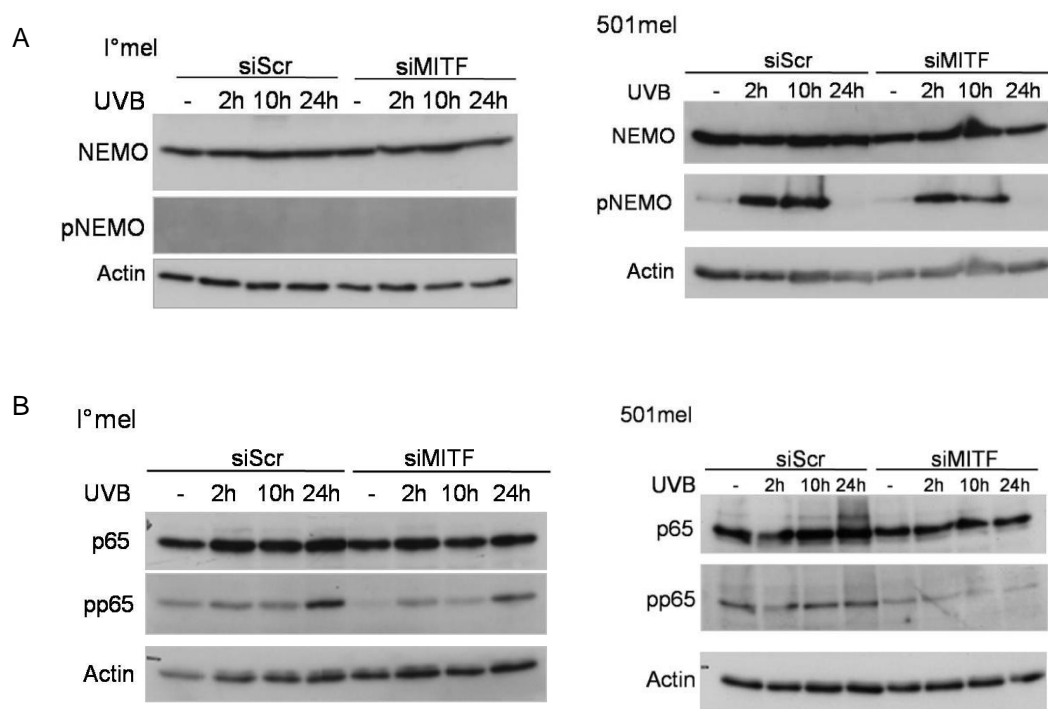


Figure 20. Phosphorylation of NEMO and p65 is MITF-dependent in I°mel and 501mel cells. siMITF- or siScr-transfected I°mel cells (left panel) and 501mel cells (right panel) underwent UVR (50 J/m²). Subsequently, either NEMO and phospho-(Ser85) NEMO (A) or p65 and phospho-(Ser536) p65 (B) were tested by immunoblot. Loading control was validated by actin immunoblot.

In order to establish experimental conditions that would allow for an analysis of the phospho-NEMO/phospho-p65 axis on a single cell level axis, we utilized immunofluorescence microscopy in I°mel and 501mel cells in dependence on MITF. Figure 21 reveals a reduced p65 phospho activity and a reduction of pp65 signal in MITF-depleted I°mel cells 2 hr and 24 hr after UVB irradiation, which confirms the results obtained by Western blot.

In addition, a sample distribution-based quantitative analysis of nuclear phospho-Ser536 p65 demonstrated a significant reduction of pp65 signal under MITF-repression conditions 2 hr and 24 hr after UV treatment, which indicates a MITF-dependent activation of p65 protein (Figure 21B).

RESULTS

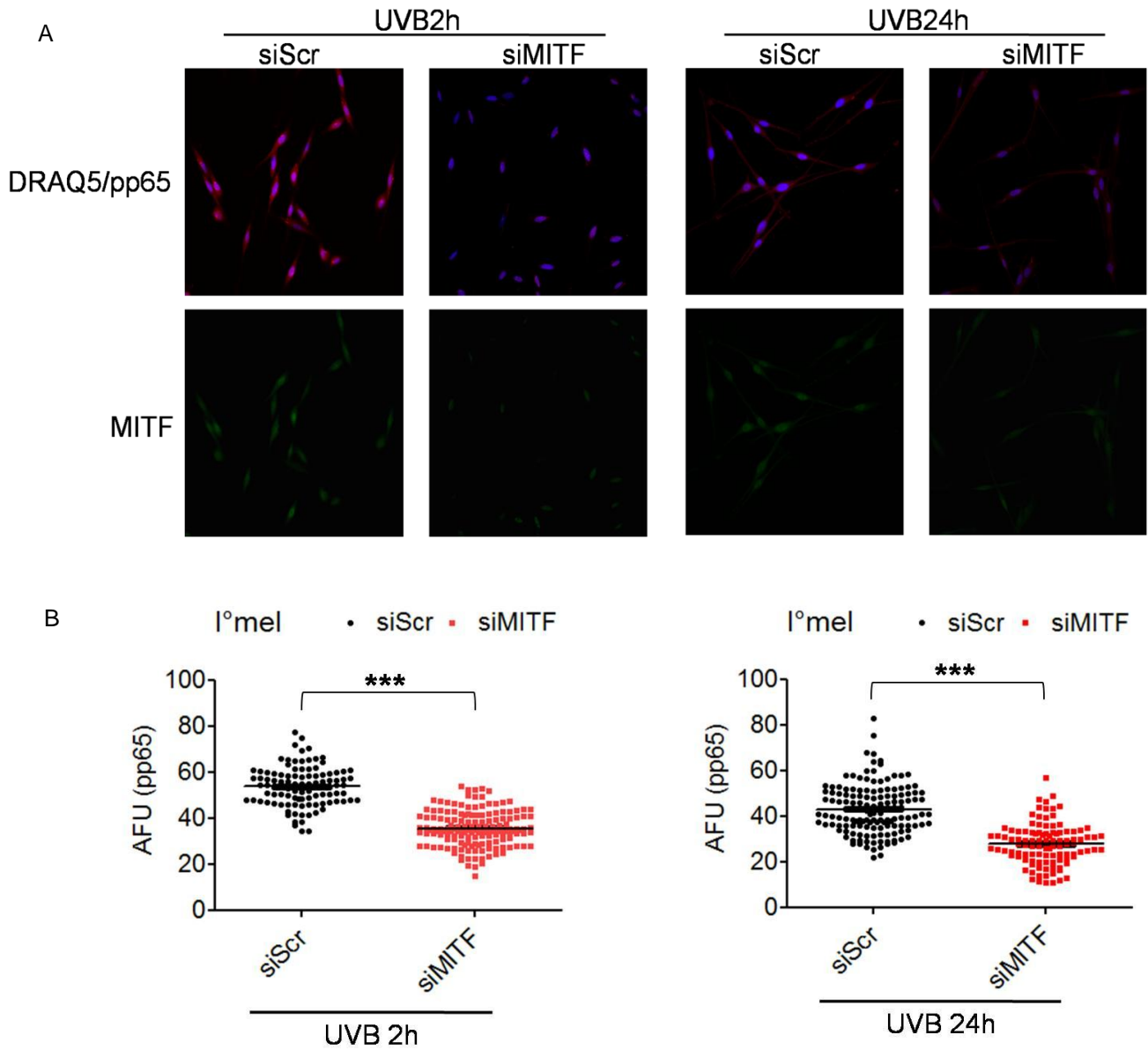


Figure 21. Detection of phospho-(Ser536) p65 in I°mel cells after UVB exposure. SiScr- and siMITF-transfected cells were irradiated with UVB (50 J/m²) and analyzed for phospho-(Ser536) p65 (red) and MITF (green) by *in situ* staining (A) and quantitative analysis (B). AFU values represent means of >100 cell nuclei (two-tailed Mann Whitney test, ***p < 0.0001). Nuclear DNA was counterstained with DRAQ5 (blue). Microscopically augmentation: x40.

RESULTS

Likewise, MITF downregulation entailed a reduction in phosphorylation of NEMO, subtly 2 hr post-UVR and hardly detectable 24 hr after UVB. Quantification of nuclear phospho-Ser85 NEMO enabled us to determine a significant reduction of nuclear pNEMO at both time points (Figure 22A and B).

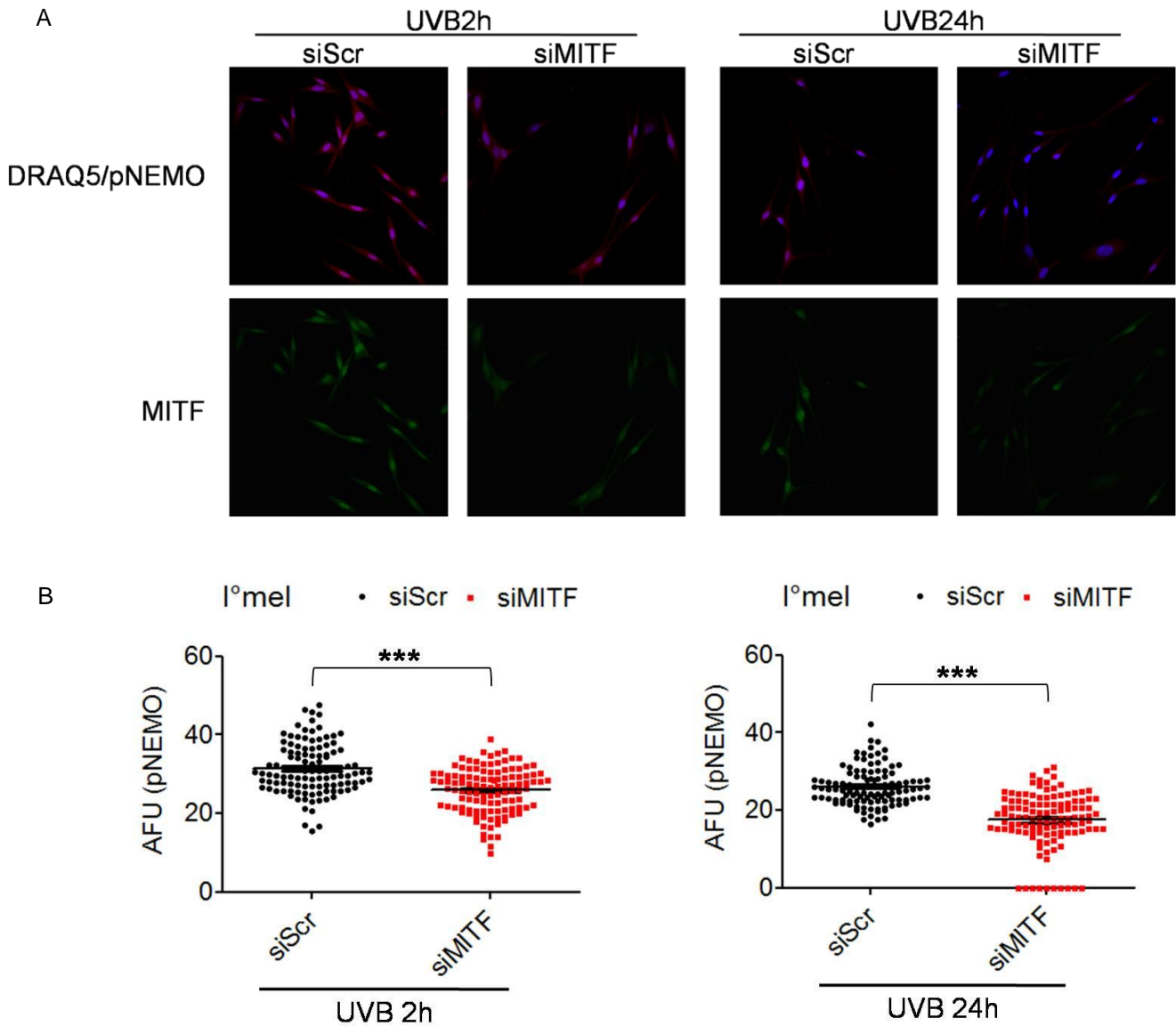


Figure 22. MITF regulates the phosphorylation and translocation into the nucleus of Ser85 NEMO under UVR in primary human melanocytes. l° mel cells were transfected with either siScr or siMITF and subsequently UVB irradiated (50 J/m^2). Cells were harvested at different time points and (A) immunolabelled with phospho-(Ser85) NEMO and MITF antibodies (red and green, respectively). DNA was counterstained with DAPI (blue). (B) Quantitative analysis of nuclear phospho-NEMO. AFU values represent means of >100 cell nuclei per sample (two-tailed Mann Whitney test, $***p < 0.0001$). Magnification factor: x40.

RESULTS

Analysis of different irradiation time points in 501mel cells revealed a weak phospho-Ser536 p65 signal in siScr control cells 10 hr after UVB exposure, minimally differing from the MITF-depleted cells (data not shown). By contrast, phospho-activation of p65 was clearly induced 24 hr post-irradiation, and a significant reduction in p65 phosphorylation was observed under MITF knockdown conditions. Quantification of nuclear phospho-p65 signal confirmed a significant decrease of pp65 in siMITF-transfected cells (Figure 23A).

Upstream regulation of NEMO was assessed with regard to MITF dependence.

Phospho-Ser85 NEMO appeared to be UV-response since irradiation of 501mel cells led to an increase of pNEMO signal. A maximum signal intensity was achieved at 24 hr post-UVR. Furthermore, quantitative analyses demonstrated a significant reduction of nuclear phospho-NEMO under MITF knockdown conditions (Figure 23B).

RESULTS

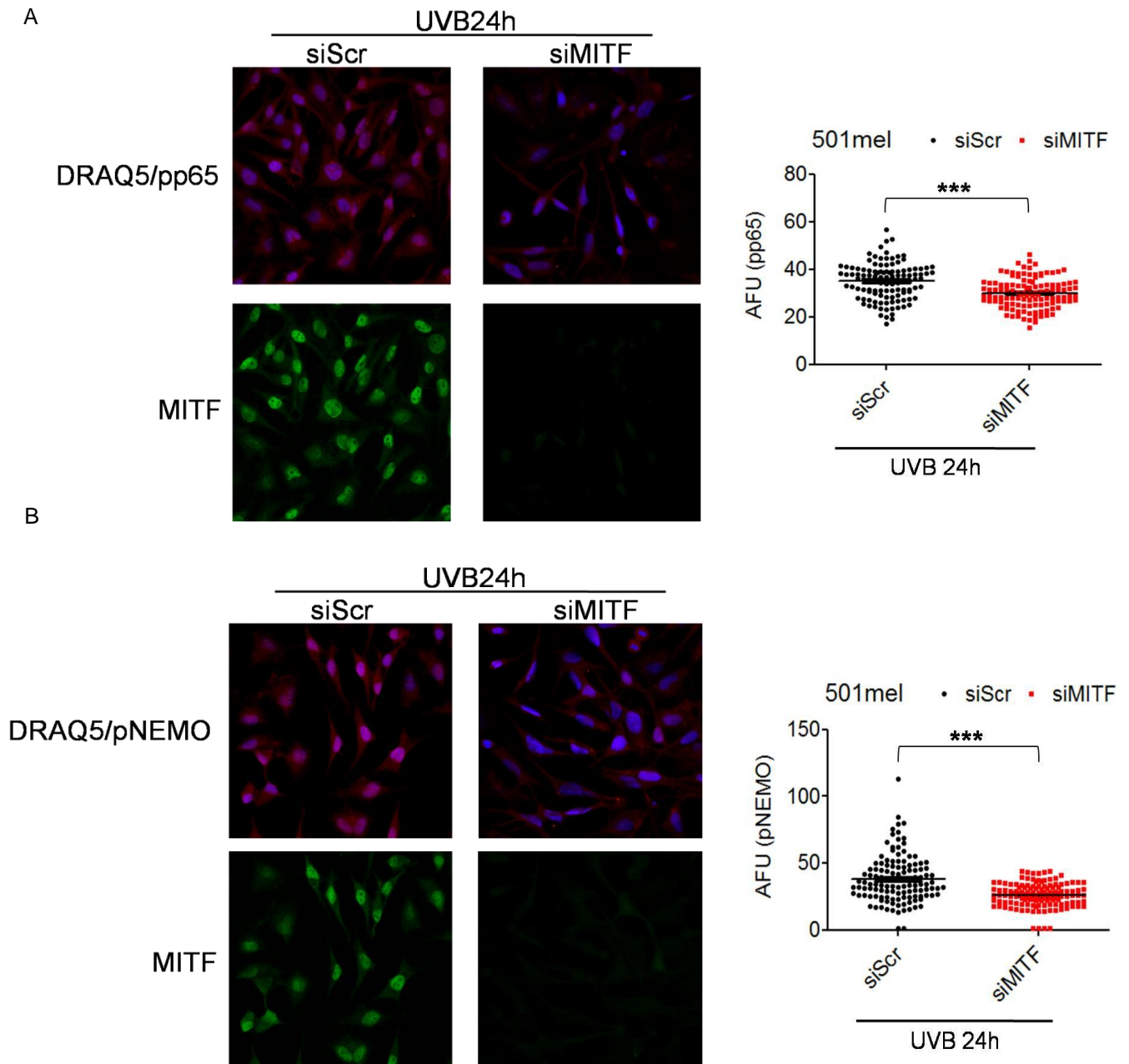


Figure 23. Phosphorylation and localization of Ser85-NEMO and Ser536-p65 in UVB irradiated 501mel cells. Detection of immunolabelled phospho-(Ser536) p65 (A) and phospho-(Ser85) NEMO (B) proteins was assessed by confocal microscopy (left panel). MITF staining (green) served as knockdown control, and DNA was counterstained with DRAQ5 (blue). (Right panel) Quantification of nuclear phospho-p65 (A) and phospho-NEMO (B) in >100 nuclei per sample were expressed by arbitrary fluorescent units, AFU (two-tailed Mann Whitney test, *** $p < 0.0001$). Microscopically augmentation: x40.

3.7 MITF plays a role in the secretion of IL8 and IL10 by regulating the transcriptional activity of these factors in 501mel cells

Several studies have identified NFκB as a family of transcription factors involved in a large variety of cellular functions including DNA damage response and the immune system. As mentioned above, UV irradiation induces an immune system response which involves numerous cytokines and chemokines [31].

Since we demonstrated a MITF-dependent regulation of p65 activation based on the decrease of phospho-(Ser536) p65 signal and of pp65 signal in the nucleus in MITF-repressed cells, we hypothesized that MITF might play an indirect role in the regulation of inflammatory reactions of the immune system in the UVR context.

In order to address this question, we analyzed the transcriptional expression of NFκB target genes encoding for inflammatory factors in primary human melanocytes and 501mel cells under MITF modulation.

From the panel of screened chemokines and cytokines, *IL8* and *IL10* revealed an MITF-dependent regulation (Figure 24 and data not shown). Intriguingly, UV irradiation led to an upregulation of *IL8* in I°mel and 501mel cells, with varying kinetics (Figure 24A left and right panel), which was significantly augmented upon MITF repression. Although IL-10 did not show UVB responsiveness, its transcriptional activity was enhanced under MITF depletion (Figure 24B). However, IL-10 mRNA was expressed at a very low level in 501mel cells, however not detectable in primary human melanocytes.

RESULTS

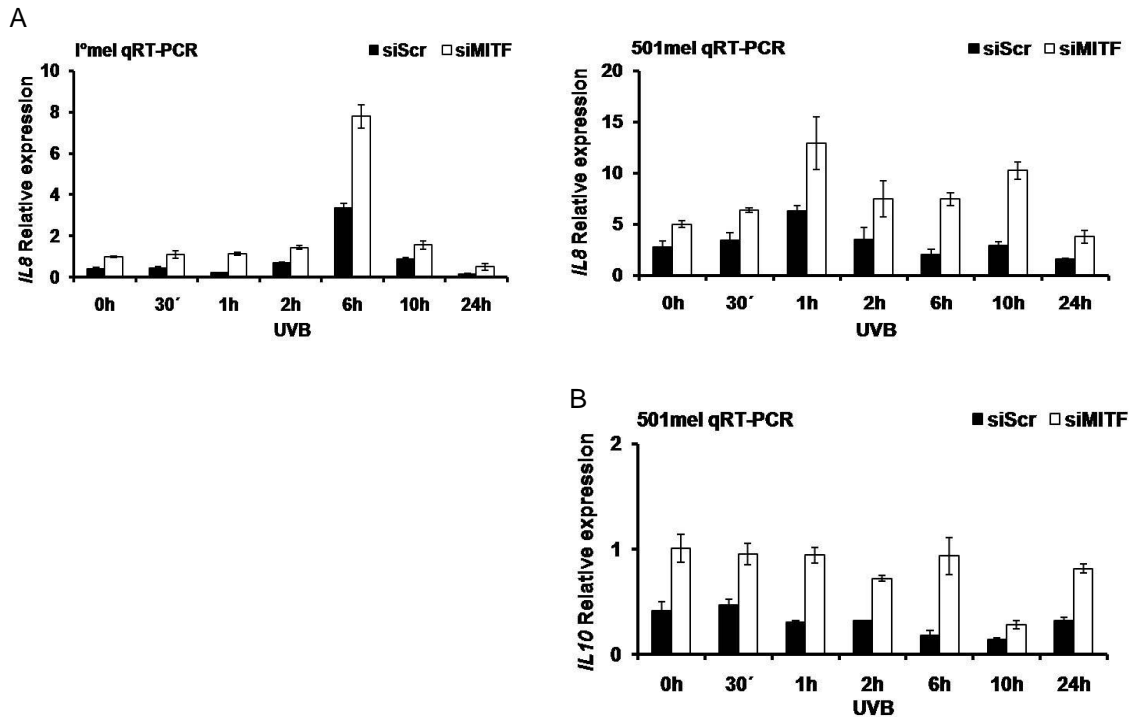


Figure 24. The transcriptional activity of *IL8* and *IL10* is MITF-dependent in I°mel and 501mel cells after UV irradiation. I°mel cells (left panel) and 501mel cells (right panel) were transfected with siScr or siMITF and UVB irradiated (50 J/m²). Relative expression of *IL8* and *IL10* (A and B, respectively) was analyzed by qRT-PCR. Error bars show the standard deviations from the mean of one out of three biological reproductions, measured in technical triplicates.

To assess the effect of MITF on functional IL8 and IL10, we proceeded analyzing the secretion of both inflammatory factors in I°mel and 501mel cells under MITF-repression by means of ELISA. Figure 25A shows partial MITF knockdown in all three biological triplicates (E1, E2 and E3) from tested 501mel cells 72 hr after UVB irradiation.

In I°mel cells, neither IL8 nor IL10 were measurable by ELISA analysis, suggesting no relevant functionality of these factors in this context or a protein abundance below the detection limit. In contrast, high amounts of IL8 were found in 501mel cell-media supernatants, further increasing over time after UV irradiation. Although this increase may be due to an additive effect, UVR could potentially also contribute to this phenomenon. siMITF transfection led to a strong increase of IL8 concentration in cellular supernatants at baseline and during the time course after UV exposure, recapitulating the results obtained by qRT-PCR (Figure 25B left panel).

In analogy to IL8, IL10 protein concentration was significantly higher in siMITF transfected cells compared to siScr control cells (Figure 25B right panel). These results would suggest a negative regulation of the pro-inflammatory cytokines IL-8

RESULTS

and IL-10 by MITF in 501 melanoma cells, which supports previous data in which MITF appears to reduce the immune system response and the invasiveness of the melanoma [63, 76].

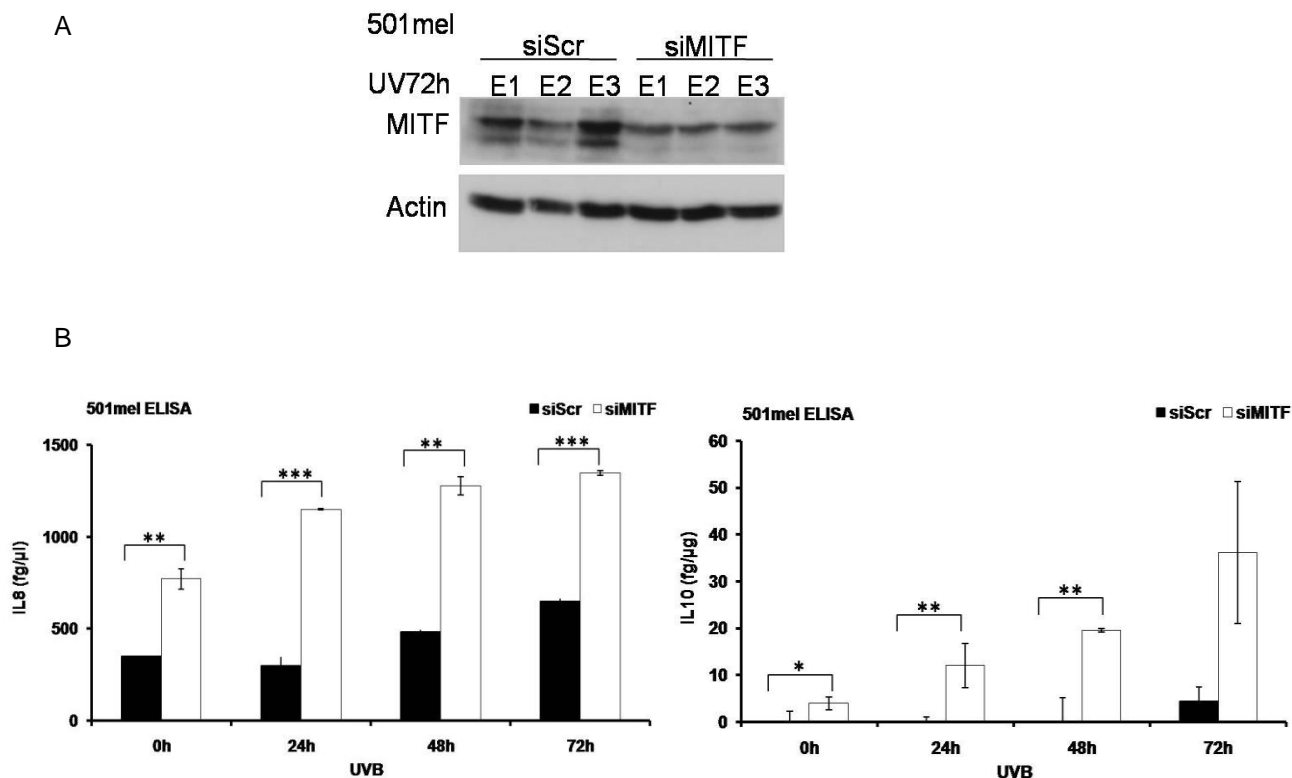


Figure 25. IL8 and IL10 dosage in 501mel cell-supernatants is regulated by MITF. 501mel cells were transfected with siRNA against MITF or siScr and subsequently irradiated with UVB (50 J/m²). (A) Confirmation of MITF knockdown was assessed by Immunoblot. Equal loading was proved by detection of actin (E1, E2 and E3 correspond to three biological triplicates). (B) Detection and quantification of secreted IL8 and IL10 were assessed by the analyses of collected supernatants at different time points by means of ELISA. Values are presented as mean +/- SD measured in biological triplicates (two-tailed Student's test; *p< 0.05, **p< 0.01, ***p< 0.001).

Presuming an MITF-dependent NFκB involvement in the regulatory mechanism of IL8 and IL10, we addressed NEMO and p65 phosphoactivity by immunoblot analysis. Under the chosen experimental conditions, the phosphorylation of NEMO and p65 were reduced under MITF knockdown (Figure 26A and B, respectively), showing a negative regulation of IL-8 and IL-10 independently of NFκB activation. These results lead to the hypothesis that the recruitment of additional transcription co-factors with phospho-(Ser 536) p65 at gene promoters may be selective upon different stimuli, defining which genes will be transcribed [113].

RESULTS

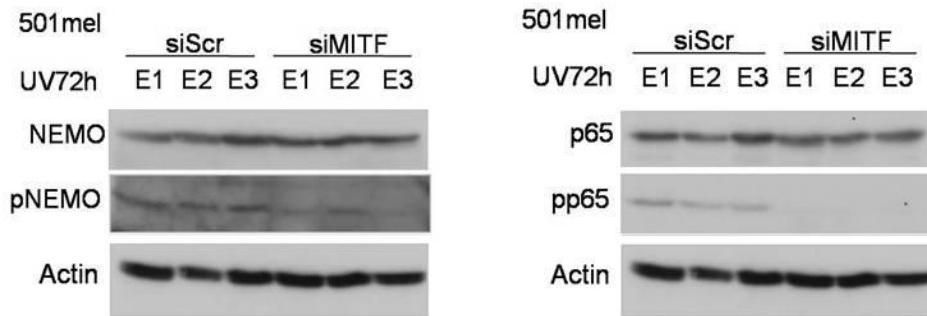


Figure 26. Protein expression and phosphorylation of (Ser 85) NEMO and (Ser 536) p65 in 501mel cells 72 hr post-irradiation. siMITF- or siScr-transfected 501mel cells were submitted to UVR (50 J/m²) and subsequently harvested 72 hr after UVB exposure. Whole protein and phospho-status of NEMO (left panel) and p65 (right panel) were assessed by Western blot. Loading control was validated by actin.

4 Discussion

In the present work, we demonstrate a specific role of MITF in the DDR through direct transcriptional regulation of XPG, which acts as a core element in NER. Furthermore, we suggest a functional link between MITF and NF κ B dependent pathways mediated by ATM, potentially extending MITF's functional repertoire to immunomodulatory processes in melanoma cells.

4.1 Nucleotide excision repair capacity of primary melanocytes and melanoma cells is dependent on MITF

The hypothesis that MITF ensures the cell's genomic integrity was built on transcriptome-wide target gene analyses [61]. Accordingly, a new model of action for MITF has recently emerged largely based on ChIPSeq data. These studies suggest direct occupancy of promoters the genes of which are involved in DNA repair including NER and BER according to gene ontology and pathway analyses [65].

In the present work, we were able to demonstrate that NER operates in an MITF-dependent manner upon UVR and cisplatin treatment. The aforementioned genotoxic procedures induce DNA adducts as the predominant type of damage which are NER system substrates. Primary human melanocytes as well as the melanoma cell lines 501mel (human) and B16V (murine) were tested for either CPDs or guanine-guanine intrastrand crosslinks after UV and cisplatin treatment, respectively. In I^o melanocytes, as well as in 501mel cells, MITF depletion led to a delayed repair kinetic of CPD lesions upon UVB exposure. In a similar manner, transient exposure of MITF-deficient I^o melanocytes and B16V cells to cisplatin resulted in a reduced DNA damage repair capacity.

Our results show, MITF's functional role in the DNA damage response, ensuring genomic stability not only in melanocytes but also in melanoma cells. We provide experimental evidence that MITF directly regulates NER through transactivation of its core element XPG. The MITF-XPG axis affects global as well as transcription-coupled repair and most importantly operates also in melanoma under genotoxic stress. Given XPG's role in DNA repair and transcription, MITF might coordinate these processes, thereby optimizing the rapid resumption of transcriptional activity after completion of strand repair. This, in turn, may have potential implications for melanoma growth and progression. A novel vitally important function of MITF has been identified in the protection against genotoxic attack, which might help explain

how melanocytes deal with the mutagenic challenge imposed by the ultraviolet radiation exposure. Furthermore, MITF's role in DNA damage repair may elucidate how the very same mechanism preserved upon cellular transformation maintains genomic stability and prevents apoptosis in melanoma by counteracting cell-intrinsic genotoxic stress as well as treatment strategies that induce a transcriptional blockade.

4.2 MITF controls DDR by direct transcriptional regulation of XPG in a lesion-specific manner.

Based on our results, which demonstrated a functional role of MITF in the DNA damage context, we were further interested in elucidating the regulatory mechanism involved in the system. Our group and others showed in the past a UV-responsiveness of MITF at both transcriptional and translational level in human primary melanocytes and implied MITF in the transcriptional regulation of genes involved in the DNA repair machinery [61, 65]. In order to establish a mechanistic link between MITF activation and the nucleotide excision repair system, we focused on one of its core elements, the endonuclease XPG which had been suggested as a potentially direct target gene of MITF in previous studies.

Exposure of several melanoma cell lines to a variety of DNA damaging agents, which involves different DNA damage repair mechanisms, led to an induction of MITF. In UVR- and cisplatin-treated cells, this induction could be linked to an enhanced DNA damage repair efficiency. Under exposure of paclitaxel, etoposide or γ -irradiation, induction of MITF might occur either to activate the DDR or, as a pro-survival factor, to prevent genotoxin-induced apoptosis. In order to elucidate MITF's role in the different genotoxic contexts, DNA damage repair assays might be performed in the future.

Intriguingly, only those cells which were treated with UVR exhibited an MITF-dependent upregulation of XPG, whereas cisplatin, carboplatin and γ -irradiation led to a XPG transactivation independently of MITF expression. These results suggest a complex coregulation of XPG by alternative transcription factors. Furthermore, we demonstrate an XPG upregulation in different genotoxic scenarios, supporting its role in additional DNA damage repair systems such as BER [114].

4.3 MITF regulates ATM upon UV irradiation

Genotoxic attack entails a complex DNA damage response, which is dependent on so-called “sensor factors” such as ATM, ATR and DNA-PK [115]. The present work suggests an MITF-dependent upregulation of ATM in primary human melanocytes. Likewise, this effect was also observed in 501mel cells, confirming previous data presented by Beuret et al [116]. Conservation of the MITF-ATM regulatory mechanism upon transformation would partially explain the high DNA repair capacity of the melanoma cells presented here.

ATM mediates NEMO activation thereby phosphorylating NEMO at Ser85, upon genotoxic attack [86, 96, 117-118]. Our results recapitulating ATM-dependent NEMO phosphorylation upon UVR, and the above mentioned regulation of ATM by MITF led us to hypothesize of a molecular link between MITF and NFκB, mediated by the activation of NEMO.

4.4 Regulation of NFκB (p65) activation by MITF is partially dependent of ser85 NEMO phosphorylation.

Previous data and this work demonstrate a regulation of members of the NFκB family by MITF. Bertolotto and coworkers described in 2011 a novel SUMOylation defective MITF mutation responsible for the upregulation of a gene set involved in the activation of NFκB signaling pathway. Additionally, E-box sequences were identified in p65/RelA and NEMO promoters, suggesting that MITF may regulate both factors at the transcriptional level. However, since MITF did not show a transcriptional regulation of neither p65 nor NEMO, we postulated a posttranslational modulation of NFκB activity by MITF. Hence, our results suggest a MITF-dependency of p65 activation in melanocytes and melanoma cells and a clear regulation of NEMO activation in 501mel cells in UVR context.

An additional “marker” for NFκB activity is the subcellular localization of p65 and NEMO. Immunofluorescence-based microscopy analyses demonstrated a reduced nuclear phospho-p65 and -NEMO under MITF knockdown conditions. As suggested above, MITF regulation on p65 phosphorylation may be an indirect effect mediated by ATM-dependent NEMO activation upon UV treatment (Figure 27). In order to confirm that p65 activation under UVR is mediated by a MITF-ATM-NEMO axis, rescue experiments in which MITF-deficient cells express recombinant NEMO could be informative.

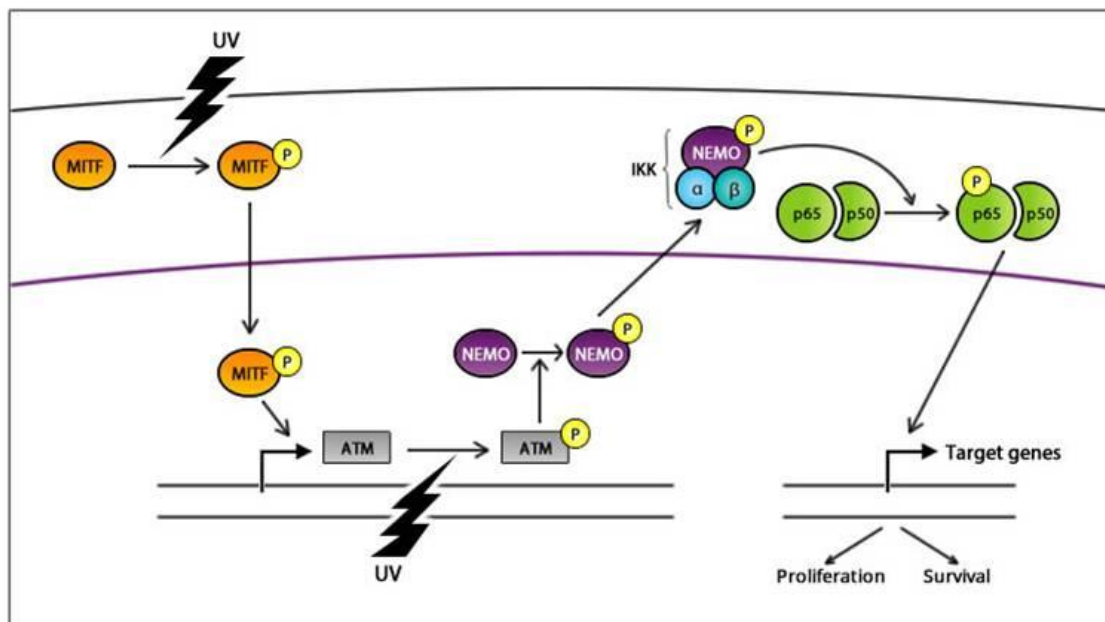


Figure 27. Overview of UV-induced NFκB signaling pathway.

An alternative hypothesis regarding the regulation of p65 activation by MITF might be an MITF-dependent induction of an alternative kinase that targets NFκB. We investigated the transcriptional and translational activity of IKKβ, a kinase subunit of the IKK signalosome, under MITF knock-down conditions. Neither in I° melanocytes nor in melanoma cells an MITF-dependency of *IKKβ* transcription was observed. For this reason, we further analyzed a potential (post)-translational regulation of IKKβ by MITF. However, no IKKβ protein could be detected, probably due to low protein abundance.

In the future, casein kinase II (CKII) should be investigated, which might explain alternative regulatory mechanisms of NFκB in dependency of MITF. CKII is UV responsive and it induces NFκB activation. Additionally, as well as MITF, CKII has been implied in cell differentiation, proliferation and apoptosis [119-120]. Interestingly, CKII regulates substrates upstream from MITF, such as β-catenin, AKT and PTEN, suggesting a role of this kinase in the MITF signaling pathway [121-123].

4.5 Expression of IL-8 and IL-10 is negatively regulated by MITF

The above mentioned results demonstrate a regulation of p65 and NEMO activation by MITF which suggests a MITF role in inflammation. Upon sun exposure, the regulation of cytokine- and chemokine-production results from an orchestrated cell-cell network with a unique goal: removal of damaged cells and reconstitution of the cellular system. Several of these immune factors, including IL-8, TNF- α , IL-1, IL-10, IL-6 and RANTES, have been identified to be regulated by NF κ B, namely, the p65/p50 heterodimer, following the canonical pathway [50]. Although there is evidence that activation of NF κ B under genotoxic stress is IKK signalosome-independent, there is also proof of an additional IKK-dependent NF κ B induction in cells exposed to genotoxic agents [96]. Our results suggesting a MITF-dependency of NF κ B phosphorylation via an ATM-NEMO axis led us to speculate about a regulation of inflammatory factors by the melanocytic-specific transcription factor. Against our assumption of a positive MITF-mediated regulation of NF κ B dependent cytokines the secretion of IL-8 and IL-10 was paradoxically enhanced upon MITF depletion. In contrast, these inflammatory factors were not detectable in 1^o melanocytes, supporting the relevance of inflammation to the development and growth of melanoma [124-125].

One explanation for the negative transcriptional regulation of IL-8 and IL-10 by MITF could be that MITF mediates the regulation on inflammatory factors partly decoupled from NF κ B signaling. This idea is supported by the results obtained by Bertolotto et al. [63], in which the novel SUMOylation-defective MITF, which leads to an activated form of MITF protein in melanoma and renal carcinoma, downregulates IL-6, a pro-inflammatory cytokine, whereas leads to the upregulation of genes associated with the activation of NF κ B pathway. Nevertheless this study, together with other groups, supports an alternative hypothesis. MITF-mediated activation of p65 could selectively activate the transcriptional expression of a certain set of genes upon UVR. In line to this notion, several groups have shown that phospho-(Ser 536) p65 selectively induces the expression of genes such as IL-8, I κ B α , RANTES and M-CSF in dependence of its dimer composition, which is determined by several factors, including stimuli and availability of the other NF κ B members. Notably, little is known about the effects of additional phosphorylations in p65, which may modulate the effect of Ser 536 phosphorylation on p65 [113, 126].

DISCUSSION

This regulatory mechanism would be in accordance with a recent model suggesting two subpopulations within a melanoma, on one hand, a group of high expressing-MITF cells, which would be responsible for the transformation and development of melanoma, and on the other hand, a low expressing-MITF subpopulation, accounting for a different phenotype signature involved in melanoma invasiveness [65]. One could assume that, in the latter cell group, MITF's decreased expression would lead to an increased immune-factor production related to motility and migration, such as IL-8 which plays a role not only as chemoattractant of immune cells, but also in promoting angiogenesis. IL-10 would support the effect of IL-8, enhancing its mRNA expression and subsequent release [31].

In conclusion, MITF would adopt a key role in fine tuning differential NFkB actions, either promoting an anti-apoptotic and proliferating program (which maintains genomic integrity), or an invasiveness phenotype associated with lower genomic stability.

5 SUMMARY

MITF-M is a melanocytic lineage-specific transcription factor involved in survival, proliferation, differentiation, genomic stability and inflammation.

Previous data demonstrated a UV- and cisplatin-induction of MITF and its direct target gene XPG, a protein involved in the NER machinery. So far, little is known about the functional role of MITF in the DNA damage repair and its regulatory mechanism. The present work shows that, in primary human melanocytes as well as in melanoma cells, UV- and cisplatin-induced MITF enhances DNA damage repair efficiency. Furthermore, we could demonstrate that MITF-dependent upregulation of XPG operates in a lesion-specific manner, involving the NER system. These results provide a better understanding of melanoma biology and reveal a MITF-dependent DNA damage response involving additional factors beside XPG which should be investigated.

In addition, our results demonstrate that, upon UVR, the activation of NEMO (a regulator of p65) and p65 itself (a subunit of the NF κ B protein family) is dependent on MITF expression. This regulation may be partially mediated by MITF-dependent ATM (trans-) activation, a sensor for DSB and UVR and activator of the NF κ B pathway. Furthermore, we show that MITF-depletion leads to upregulation of IL-8 and IL-10 in human melanoma cells (presumably by the MITF-mediated regulation of p65 post-translational modification). More detailed expression analyses of IL-8 and IL-10 in the context of MITF-p65 axis should be performed in order to better understand the immunological aspects of melanoma biology. Given the role of IL-8 and IL-10 in inflammation, angiogenesis and migration, cytotoxic assays as well as invasion experiments should be performed upon MITF-depletion, elucidating whether MITF plays a role in immune system response and invasiveness of melanoma.

Our results support a model in which MITF plays a crucial role in DNA damage repair involving NER, by the regulation of XPG upon UVR. Furthermore, we suggest an MITF-mediated link between DNA damage response and inflammation, regulating the inflammatory factors IL-8 and IL-10.

6 ZUSAMMENFASSUNG

MITF-M ist ein melanozyten-spezifischer Transkriptionsfaktor, der biologische Funktionen wie Überleben, Proliferation, Differenzierung, genomische Stabilität und Entzündungsprozesse reguliert.

Obwohl bekannt ist, dass sowohl MITF als auch sein direktes Zielgen XPG durch UV- oder Cisplatin-induzierte DNA-Schäden in ihrer Expression induziert werden, war die präzise Rolle von MITF in der DNA-Schadensreparatur bislang noch nicht aufgeklärt worden. Die vorliegende Arbeit zeigt zum ersten Mal, dass UV- und Cisplatin induziertes MITF sowohl in primären Melanozyten, als auch in Melanomzellen die Effizienz der DNA-Schadensreparatur verstärkt. Zudem konnte gezeigt werden, dass die MITF-abhängige Induktion von XPG nur im Rahmen des UV-aktivierten Nukleotid-Exzisions-Reparatur (NER)- Systems zu beobachten ist.

Darüberhinaus konnte eine MITF-vermittelte Aktivierung der NFkB-Untereinheiten NEMO und p65 nachgewiesen werden, die teilweise durch die (Trans-)Aktivierung von ATM (ein DSB- und UVR-Sensor und Aktivator des NFkB Signalwegs) in Abhängigkeit von MITF zu erklären ist. Schließlich wurde eine durch Depletion von MITF induzierte Induktion der Entzündungsmediatoren IL-8 und IL-10 beobachtet. Zusammengefasst unterstützen unsere Ergebnisse ein Modell, in dem MITF eine essenzielle Rolle in der NER-basierten Reparatur zukommt, welche es durch Regulation des Reparaturfaktors XPG ausübt. Darüberhinaus deuten die Ergebnisse darauf hin, dass MITF ein Bindeglied zwischen der DNA-Schadensantwort und der inflammatorischen Reaktion darstellt.

Aufbauend auf diesen Untersuchungen, könnte die Analyse weiterer Faktoren, die in der MITF-abhängigen DNA-Schadensantwort eine Rolle spielen, in Zukunft zu einem besseren Verständnis der Biologie des Melanoms und seiner Interaktion mit dem Immunsystem führen.

7 LIST OF ABBREVIATIONS

α -MSH	Melanocyte-stimulating hormone alpha
A	Adenosin
ACTH	Adrenocorticotropin
ATM	Ataxia telangiectasia mutated
ATR	ATM and Rad3 Related
bFGF	(human) basic Fibroblast Growth Factor
bHLH-LZ	basic helix-loop-helix-leucine zipper
BER	Base- Excision Repair
BPE	Bovine Pituitary Extract
Br- dUTP	Bromol Desoxyuridine Triphosphat
C	Cytosin
cAMP	cyclic Adenosine Monophosphat
CAPS	<i>N</i> -cyclohexyl-3-aminopropanesulfonic acid
CBP	CREB-binding protein
CD95	Cluster of differentiation 95
CDK2	Cyclin Dependant Kinase 2
cDNA	complementary DNA
CPD	Cyclobutan Pyrimidin Dimer
CRE	cAMP responsiveness element
CREB	cAMP response element-binding protein
CS	Cockayne syndrome
Ct	cycle threshold
DDR	DNA damage response
DMSO	Dimethyl sulfoxid
DNA	Desoxyribonucleic acid
DRAQ5	1, 5-bis{[2-(di-methylamino)ethyl]amino}-4, 8-dihydroxyanthracene-9, 10-dione
ECL	Enhanced chemiluminescence
EDTA	Ethylenediaminetetraacetic acid
ELISA	Enzyme Linked Immunosorbent Assay
ERK	Extracellular-signal-regulated kinase
FACS	Fluorescence- activated Cell Sorting
FBS (FCS)	Fetal bovine serum

LIST OF ABBREVIATIONS

G	Guanosine
HRP	Horseradish peroxidase
IF	Immunofluorescence
IgG	Immunoglobulin G
I κ B	Inhibitor of κ B
IKK	I κ B kinase
J	Joule
μ	micro
m	milli
M	Molar
MAPK	Mitogen-activated protein kinase
MC1R	Melanocrotin Receptor 1
MITF	Microphthalmia-associated transcription factor
MMR	Mismatch Repair
mRNA	messenger RNA
n	nano
NEMO	NF κ B essential modulator
NER	Nucleotide Excision Repair
NHEJ	Non- Homologous End Joining
NF κ B	Nuclear factor kappa-light-chain-enhancer of activated b-cells
NIK	NF κ B inducing kinase
NLS	Nuclear localization signal
PAGE	Polyacrylamide gel electrophoresis
PBS	Phosphate Buffered Saline
PCR	Polymerase Chain Reaction
Pen/Strep	Penicillin/Streptomycin
PKA	Protein Kinase A
PMSF	Phenylmethylsulfonyl fluoride
pNEMO	phospho (Ser85) NEMO
POMC	Pro-opiomelanocortin
pp65	phospho (Ser536) p65
Pp90rsk	90-kDa ribosomal S6 kinase
RHD	Rel homology domain
RNA	Ribonucleic acid

LIST OF ABBREVIATIONS

rpm	rotation per minute
RT-PCR	Real time-PCR
SCF	Stem cell factor
SDS	Sodium dodecyl sulfate
siMITF	MITF siRNA
siRNA	small interfering RNA
siScr	Scramble siRNA
T	Thymidine
TAD	Transactivation domain
TBS	Tris-buffered saline
TEMED	, <i>N,N,N</i> -Tetramethyl-ethane-1,2-diamine
TPA	12- O- Tetradecanoylphorbol 13- acetate
Tris	2-Amino-2-hydroxymethyl-propane-1,3-diol
TYR	Tyrosinase
TYRP1	Tyrosinase Related Protein 1
U	Uridine
UV	Ultraviolet
UVR	UV radiation
WB	Western blot
WS2A	Waardenburg syndrome type IIa
XP	Xeroderma Pigmentosum
XPG	Xeroderma Pigmentosum Complementation Group C

8 REFERENCES

1. Barden, H. and S. Levine, *Histochemical observations on rodent brain melanin*. Brain Res Bull, 1983. **10**(6): p. 847-51.
2. Markert, C.L. and W.K. Silvers, *The Effects of Genotype and Cell Environment on Melanoblast Differentiation in the House Mouse*. Genetics, 1956. **41**(3): p. 429-50.
3. Theriault, L.L. and L.S. Hurley, *Ultrastructure of developing melanosomes in C57 black and pallid mice*. Dev Biol, 1970. **23**(2): p. 261-75.
4. Plettenberg, A., et al., *Human melanocytes and melanoma cells constitutively express the Bcl-2 proto-oncogene in situ and in cell culture*. Am J Pathol, 1995. **146**(3): p. 651-9.
5. Slominski, A., R. Paus, and D. Schadendorf, *Melanocytes as "sensory" and regulatory cells in the epidermis*. J Theor Biol, 1993. **164**(1): p. 103-20.
6. Kock, A., et al., *Cytokines and human malignant melanoma. Immuno- and growth-regulatory peptides in melanoma biology*. Cancer Treat Res, 1991. **54**: p. 41-66.
7. Dianov, G.L., et al., *Single nucleotide patch base excision repair is the major pathway for removal of thymine glycol from DNA in human cell extracts*. J Biol Chem, 2000. **275**(16): p. 11809-13.
8. Shuck, S.C., E.A. Short, and J.J. Turchi, *Eukaryotic nucleotide excision repair: from understanding mechanisms to influencing biology*. Cell Res, 2008. **18**(1): p. 64-72.
9. Fuss, J.O. and P.K. Cooper, *DNA repair: dynamic defenders against cancer and aging*. PLoS Biol, 2006. **4**(6): p. e203.
10. Chakraborty, A.K., et al., *Production and release of proopiomelanocortin (POMC) derived peptides by human melanocytes and keratinocytes in culture: regulation by ultraviolet B*. Biochim Biophys Acta, 1996. **1313**(2): p. 130-8.
11. Suzuki, I., et al., *Binding of melanotropic hormones to the melanocortin receptor MC1R on human melanocytes stimulates proliferation and melanogenesis*. Endocrinology, 1996. **137**(5): p. 1627-33.
12. Levy, C., M. Khaled, and D.E. Fisher, *MITF: master regulator of melanocyte development and melanoma oncogene*. Trends Mol Med, 2006. **12**(9): p. 406-14.
13. Miller, A.J. and H. Tsao, *New insights into pigmentary pathways and skin cancer*. Br J Dermatol, 2010. **162**(1): p. 22-8.
14. Valverde, P., et al., *Variants of the melanocyte-stimulating hormone receptor gene are associated with red hair and fair skin in humans*. Nat Genet, 1995. **11**(3): p. 328-30.
15. Flanagan, N., et al., *Pleiotropic effects of the melanocortin 1 receptor (MC1R) gene on human pigmentation*. Hum Mol Genet, 2000. **9**(17): p. 2531-7.
16. Tsatmali, M., et al., *alpha-melanocyte-stimulating hormone modulates nitric oxide production in melanocytes*. J Invest Dermatol, 2000. **114**(3): p. 520-6.
17. Bohm, M., et al., *alpha-Melanocyte-stimulating hormone protects from ultraviolet radiation-induced apoptosis and DNA damage*. J Biol Chem, 2005. **280**(7): p. 5795-802.
18. Dong, L., et al., *Melanocyte-stimulating hormone directly enhances UV-Induced DNA repair in keratinocytes by a xeroderma pigmentosum group A-dependent mechanism*. Cancer Res, 2010. **70**(9): p. 3547-56.

REFERENCES

19. Catania, A. and J.M. Lipton, *alpha-Melanocyte stimulating hormone in the modulation of host reactions*. *Endocr Rev*, 1993. **14**(5): p. 564-76.
20. Kupper, T.S. and R.C. Fuhlbrigge, *Immune surveillance in the skin: mechanisms and clinical consequences*. *Nat Rev Immunol*, 2004. **4**(3): p. 211-22.
21. Das, P.K., et al., *A symbiotic concept of autoimmunity and tumour immunity: lessons from vitiligo*. *Trends Immunol*, 2001. **22**(3): p. 130-6.
22. Chen, G. and D.V. Goeddel, *TNF-R1 signaling: a beautiful pathway*. *Science*, 2002. **296**(5573): p. 1634-5.
23. Mukaida, N. and K. Matsushima, *Regulation of IL-8 production and the characteristics of the receptors for IL-8*. *Cytokines*, 1992. **4**: p. 41-53.
24. Oppenheim, J.J., et al., *Properties of the novel proinflammatory supergene "intercrine" cytokine family*. *Annu Rev Immunol*, 1991. **9**: p. 617-48.
25. Strieter, R.M., et al., *Endothelial cell gene expression of a neutrophil chemotactic factor by TNF-alpha, LPS, and IL-1 beta*. *Science*, 1989. **243**(4897): p. 1467-9.
26. Mori, N. and D. Prager, *Transactivation of the interleukin-1alpha promoter by human T-cell leukemia virus type I and type II Tax proteins*. *Blood*, 1996. **87**(8): p. 3410-7.
27. Wood, P.L., *Differential regulation of IL-1 alpha and TNF alpha release from immortalized murine microglia (BV-2)*. *Life Sci*, 1994. **55**(9): p. 661-8.
28. Kunsch, C. and C.A. Rosen, *NF-kappa B subunit-specific regulation of the interleukin-8 promoter*. *Mol Cell Biol*, 1993. **13**(10): p. 6137-46.
29. Kunsch, C., et al., *Synergistic transcriptional activation of the IL-8 gene by NF-kappa B p65 (RelA) and NF-IL-6*. *J Immunol*, 1994. **153**(1): p. 153-64.
30. Saraiva, M. and A. O'Garra, *The regulation of IL-10 production by immune cells*. *Nat Rev Immunol*, 2010. **10**(3): p. 170-81.
31. Scholzen, T., et al., *Ultraviolet light and interleukin-10 modulate expression of cytokines by transformed human dermal microvascular endothelial cells (HMEC-1)*. *J Invest Dermatol*, 1998. **111**(1): p. 50-6.
32. Jerant, A.F., et al., *Early detection and treatment of skin cancer*. *Am Fam Physician*, 2000. **62**(2): p. 357-68, 375-6, 381-2.
33. Clark, W.H., Jr., et al., *A study of tumor progression: the precursor lesions of superficial spreading and nodular melanoma*. *Hum Pathol*, 1984. **15**(12): p. 1147-65.
34. Breslow, A., *Thickness, cross-sectional areas and depth of invasion in the prognosis of cutaneous melanoma*. *Ann Surg*, 1970. **172**(5): p. 902-8.
35. Jemal, A., et al., *Cancer statistics, 2003*. *CA Cancer J Clin*, 2003. **53**(1): p. 5-26.
36. Miller, A.J. and M.C. Mihm, Jr., *Melanoma*. *N Engl J Med*, 2006. **355**(1): p. 51-65.
37. Hocker, T. and H. Tsao, *Ultraviolet radiation and melanoma: a systematic review and analysis of reported sequence variants*. *Hum Mutat*, 2007. **28**(6): p. 578-88.
38. Davies, H., et al., *Mutations of the BRAF gene in human cancer*. *Nature*, 2002. **417**(6892): p. 949-54.
39. Emery, C.M., et al., *MEK1 mutations confer resistance to MEK and B-RAF inhibition*. *Proc Natl Acad Sci U S A*, 2009. **106**(48): p. 20411-6.

REFERENCES

40. Tsao, H., et al., *Identification of PTEN/MMAC1 alterations in uncultured melanomas and melanoma cell lines*. *Oncogene*, 1998. **16**(26): p. 3397-402.
41. Omholt, K., et al., *Mutations of PIK3CA are rare in cutaneous melanoma*. *Melanoma Res*, 2006. **16**(2): p. 197-200.
42. Rakosy, Z., et al., *Characterization of 9p21 copy number alterations in human melanoma by fluorescence in situ hybridization*. *Cancer Genet Cytogenet*, 2008. **182**(2): p. 116-21.
43. Goldstein, A.M., et al., *Features associated with germline CDKN2A mutations: a GenoMEL study of melanoma-prone families from three continents*. *J Med Genet*, 2007. **44**(2): p. 99-106.
44. Smalley, K.S., et al., *Identification of a novel subgroup of melanomas with KIT/cyclin-dependent kinase-4 overexpression*. *Cancer Res*, 2008. **68**(14): p. 5743-52.
45. Yang, G., A. Rajadurai, and H. Tsao, *Recurrent patterns of dual RB and p53 pathway inactivation in melanoma*. *J Invest Dermatol*, 2005. **125**(6): p. 1242-51.
46. Friedberg, E.C., *How nucleotide excision repair protects against cancer*. *Nat Rev Cancer*, 2001. **1**(1): p. 22-33.
47. Abdel-Malek, Z.A., et al., *The melanocortin 1 receptor and the UV response of human melanocytes--a shift in paradigm*. *Photochem Photobiol*, 2008. **84**(2): p. 501-8.
48. Lorigan, P., T. Eisen, and A. Hauschild, *Systemic therapy for metastatic malignant melanoma--from deeply disappointing to bright future?* *Exp Dermatol*, 2008. **17**(5): p. 383-94.
49. Balch, C.M., et al., *Final version of 2009 AJCC melanoma staging and classification*. *J Clin Oncol*, 2009. **27**(36): p. 6199-206.
50. Hersh, E.M., et al., *A phase 2 clinical trial of nab-paclitaxel in previously treated and chemotherapy-naive patients with metastatic melanoma*. *Cancer*, 2010. **116**(1): p. 155-63.
51. Ueda, Y. and A. Richmond, *NF-kappaB activation in melanoma*. *Pigment Cell Res*, 2006. **19**(2): p. 112-24.
52. Strumberg, D., *Preclinical and clinical development of the oral multikinase inhibitor sorafenib in cancer treatment*. *Drugs Today (Barc)*, 2005. **41**(12): p. 773-84.
53. Tsai, J., et al., *Discovery of a selective inhibitor of oncogenic B-Raf kinase with potent antimelanoma activity*. *Proc Natl Acad Sci U S A*, 2008. **105**(8): p. 3041-6.
54. Flaherty, K.T., et al., *Inhibition of mutated, activated BRAF in metastatic melanoma*. *N Engl J Med*, 2010. **363**(9): p. 809-19.
55. Pratilas, C.A., F. Xing, and D.B. Solit, *Targeting oncogenic BRAF in human cancer*. *Curr Top Microbiol Immunol*, 2012. **355**: p. 83-98.
56. Atchley, W.R. and W.M. Fitch, *A natural classification of the basic helix-loop-helix class of transcription factors*. *Proc Natl Acad Sci U S A*, 1997. **94**(10): p. 5172-6.
57. Hemesath, T.J., et al., *microphthalmia, a critical factor in melanocyte development, defines a discrete transcription factor family*. *Genes Dev*, 1994. **8**(22): p. 2770-80.
58. Saito, H., et al., *Melanocyte-specific microphthalmia-associated transcription factor isoform activates its own gene promoter through physical interaction with lymphoid-enhancing factor 1*. *J Biol Chem*, 2002. **277**(32): p. 28787-94.

REFERENCES

59. Opdecamp, K., et al., *Melanocyte development in vivo and in neural crest cell cultures: crucial dependence on the Mitf basic-helix-loop-helix-zipper transcription factor*. Development, 1997. **124**(12): p. 2377-86.
60. Tachibana, M., *MITF: a stream flowing for pigment cells*. Pigment Cell Res, 2000. **13**(4): p. 230-40.
61. McGill, G.G., et al., *Bcl2 regulation by the melanocyte master regulator Mitf modulates lineage survival and melanoma cell viability*. Cell, 2002. **109**(6): p. 707-18.
62. Loercher, A.E., et al., *MITF links differentiation with cell cycle arrest in melanocytes by transcriptional activation of INK4A*. J Cell Biol, 2005. **168**(1): p. 35-40.
63. Bertolotto, C., et al., *A SUMOylation-defective MITF germline mutation predisposes to melanoma and renal carcinoma*. Nature, 2011. **480**(7375): p. 94-8.
64. Yokoyama, S., et al., *A novel recurrent mutation in MITF predisposes to familial and sporadic melanoma*. Nature, 2011. **480**(7375): p. 99-103.
65. Strub, T., et al., *Essential role of microphthalmia transcription factor for DNA replication, mitosis and genomic stability in melanoma*. Oncogene, 2011. **30**(20): p. 2319-32.
66. Hocker, T.L., M.K. Singh, and H. Tsao, *Melanoma genetics and therapeutic approaches in the 21st century: moving from the benchside to the bedside*. J Invest Dermatol, 2008. **128**(11): p. 2575-95.
67. Bertolotto, C., et al., *Microphthalmia gene product as a signal transducer in cAMP-induced differentiation of melanocytes*. J Cell Biol, 1998. **142**(3): p. 827-35.
68. Takeda, K., et al., *Induction of melanocyte-specific microphthalmia-associated transcription factor by Wnt-3a*. J Biol Chem, 2000. **275**(19): p. 14013-6.
69. Pingault, V., et al., *SOX10 mutations in patients with Waardenburg-Hirschsprung disease*. Nat Genet, 1998. **18**(2): p. 171-3.
70. Tassabehji, M., et al., *Mutations in the PAX3 gene causing Waardenburg syndrome type 1 and type 2*. Nat Genet, 1993. **3**(1): p. 26-30.
71. Baldwin, C.T., et al., *Mutations in PAX3 that cause Waardenburg syndrome type I: ten new mutations and review of the literature*. Am J Med Genet, 1995. **58**(2): p. 115-22.
72. Lin, J.Y. and D.E. Fisher, *Melanocyte biology and skin pigmentation*. Nature, 2007. **445**(7130): p. 843-50.
73. Hemesath, T.J., et al., *MAP kinase links the transcription factor Microphthalmia to c-Kit signalling in melanocytes*. Nature, 1998. **391**(6664): p. 298-301.
74. Takeda, K., et al., *Ser298 of MITF, a mutation site in Waardenburg syndrome type 2, is a phosphorylation site with functional significance*. Hum Mol Genet, 2000. **9**(1): p. 125-32.
75. Garraway, L.A., et al., *Integrative genomic analyses identify MITF as a lineage survival oncogene amplified in malignant melanoma*. Nature, 2005. **436**(7047): p. 117-22.
76. Carreira, S., et al., *Mitf regulation of Dial1 controls melanoma proliferation and invasiveness*. Genes Dev, 2006. **20**(24): p. 3426-39.

REFERENCES

77. Hoek, K.S., et al., *In vivo switching of human melanoma cells between proliferative and invasive states*. *Cancer Res*, 2008. **68**(3): p. 650-6.
78. Zotter, A., et al., *Recruitment of the nucleotide excision repair endonuclease XPG to sites of UV-induced dna damage depends on functional TFIIH*. *Mol Cell Biol*, 2006. **26**(23): p. 8868-79.
79. Lalle, P., et al., *The founding members of xeroderma pigmentosum group G produce XPG protein with severely impaired endonuclease activity*. *J Invest Dermatol*, 2002. **118**(2): p. 344-51.
80. Lee, S.K., et al., *Requirement of yeast RAD2, a homolog of human XPG gene, for efficient RNA polymerase II transcription. implications for Cockayne syndrome*. *Cell*, 2002. **109**(7): p. 823-34.
81. Hanawalt, P.C. and G. Spivak, *Transcription-coupled DNA repair: two decades of progress and surprises*. *Nat Rev Mol Cell Biol*, 2008. **9**(12): p. 958-70.
82. Lee, J.H. and T.T. Paull, *Activation and regulation of ATM kinase activity in response to DNA double-strand breaks*. *Oncogene*, 2007. **26**(56): p. 7741-8.
83. Heffernan, T.P., et al., *ATR-Chk1 pathway inhibition promotes apoptosis after UV treatment in primary human keratinocytes: potential basis for the UV protective effects of caffeine*. *J Invest Dermatol*, 2009. **129**(7): p. 1805-15.
84. Matsuoka, S., et al., *Ataxia telangiectasia-mutated phosphorylates Chk2 in vivo and in vitro*. *Proc Natl Acad Sci U S A*, 2000. **97**(19): p. 10389-94.
85. Matsuoka, S., et al., *ATM and ATR substrate analysis reveals extensive protein networks responsive to DNA damage*. *Science*, 2007. **316**(5828): p. 1160-6.
86. Miyamoto, S., *Nuclear initiated NF-kappaB signaling: NEMO and ATM take center stage*. *Cell Res*, 2011. **21**(1): p. 116-30.
87. McConville, C.M., et al., *Mutations associated with variant phenotypes in ataxia-telangiectasia*. *Am J Hum Genet*, 1996. **59**(2): p. 320-30.
88. Gilmore, T.D., *Introduction to NF-kappaB: players, pathways, perspectives*. *Oncogene*, 2006. **25**(51): p. 6680-4.
89. Perkins, N.D., *Integrating cell-signalling pathways with NF-kappaB and IKK function*. *Nat Rev Mol Cell Biol*, 2007. **8**(1): p. 49-62.
90. Ghosh, S., M.J. May, and E.B. Kopp, *NF-kappa B and Rel proteins: evolutionarily conserved mediators of immune responses*. *Annu Rev Immunol*, 1998. **16**: p. 225-60.
91. Sen, R. and D. Baltimore, *Inducibility of kappa immunoglobulin enhancer-binding protein Nf-kappa B by a posttranslational mechanism*. *Cell*, 1986. **47**(6): p. 921-8.
92. Marok, R., et al., *Activation of the transcription factor nuclear factor-kappaB in human inflamed synovial tissue*. *Arthritis Rheum*, 1996. **39**(4): p. 583-91.
93. Neurath, M.F., et al., *Local administration of antisense phosphorothioate oligonucleotides to the p65 subunit of NF-kappa B abrogates established experimental colitis in mice*. *Nat Med*, 1996. **2**(9): p. 998-1004.
94. DeLuca, C., et al., *Nuclear IkappaBbeta maintains persistent NF-kappaB activation in HIV-1-infected myeloid cells*. *J Biol Chem*, 1999. **274**(19): p. 13010-6.

REFERENCES

95. Patel, A., et al., *Herpes simplex type 1 induction of persistent NF-kappa B nuclear translocation increases the efficiency of virus replication*. Virology, 1998. **247**(2): p. 212-22.
96. Janssens, S. and J. Tschopp, *Signals from within: the DNA-damage-induced NF-kappaB response*. Cell Death Differ, 2006. **13**(5): p. 773-84.
97. Rosette, C. and M. Karin, *Ultraviolet light and osmotic stress: activation of the JNK cascade through multiple growth factor and cytokine receptors*. Science, 1996. **274**(5290): p. 1194-7.
98. Yarosh, D.B., et al., *Cyclobutane pyrimidine dimers in UV-DNA induce release of soluble mediators that activate the human immunodeficiency virus promoter*. J Invest Dermatol, 1993. **100**(6): p. 790-4.
99. Huang, B., et al., *Posttranslational modifications of NF-kappaB: another layer of regulation for NF-kappaB signaling pathway*. Cell Signal, 2010. **22**(9): p. 1282-90.
100. Basseres, D.S. and A.S. Baldwin, *Nuclear factor-kappaB and inhibitor of kappaB kinase pathways in oncogenic initiation and progression*. Oncogene, 2006. **25**(51): p. 6817-30.
101. Dhawan, P. and A. Richmond, *A novel NF-kappa B-inducing kinase-MAPK signaling pathway up-regulates NF-kappa B activity in melanoma cells*. J Biol Chem, 2002. **277**(10): p. 7920-8.
102. Becker, T.M., et al., *Impaired inhibition of NF-kappaB activity by melanoma-associated p16INK4a mutations*. Biochem Biophys Res Commun, 2005. **332**(3): p. 873-9.
103. Rizos, H., et al., *Mutations in the INK4a/ARF melanoma susceptibility locus functionally impair p14ARF*. J Biol Chem, 2001. **276**(44): p. 41424-34.
104. Gu, L., et al., *Identification and characterization of the IKKalpha promoter: positive and negative regulation by ETS-1 and p53, respectively*. J Biol Chem, 2004. **279**(50): p. 52141-9.
105. Singh, R.K., et al., *Expression of interleukin-8 in primary and metastatic malignant melanoma of the skin*. Melanoma Res, 1999. **9**(4): p. 383-7.
106. Hayden, M.S. and S. Ghosh, *Shared principles in NF-kappaB signaling*. Cell, 2008. **132**(3): p. 344-62.
107. Mrowietz, U., et al., *The chemokine RANTES is secreted by human melanoma cells and is associated with enhanced tumour formation in nude mice*. Br J Cancer, 1999. **79**(7-8): p. 1025-31.
108. Bloethner, S., et al., *Effect of common B-RAF and N-RAS mutations on global gene expression in melanoma cell lines*. Carcinogenesis, 2005. **26**(7): p. 1224-32.
109. Huang, S., et al., *Nuclear factor-kappaB activity correlates with growth, angiogenesis, and metastasis of human melanoma cells in nude mice*. Clin Cancer Res, 2000. **6**(6): p. 2573-81.
110. Mellon, I., et al., *Preferential DNA repair of an active gene in human cells*. Proc Natl Acad Sci U S A, 1986. **83**(23): p. 8878-82.
111. Mellon, I., G. Spivak, and P.C. Hanawalt, *Selective removal of transcription-blocking DNA damage from the transcribed strand of the mammalian DHFR gene*. Cell, 1987. **51**(2): p. 241-9.

REFERENCES

112. Sebban, H., S. Yamaoka, and G. Courtois, *Posttranslational modifications of NEMO and its partners in NF-kappaB signaling*. Trends Cell Biol, 2006. **16**(11): p. 569-77.
113. Sasaki, C.Y., et al., *Phosphorylation of RelA/p65 on serine 536 defines an I{kappa}B{alpha}-independent NF-{kappa}B pathway*. J Biol Chem, 2005. **280**(41): p. 34538-47.
114. Klungland, A., et al., *Base excision repair of oxidative DNA damage activated by XPG protein*. Mol Cell, 1999. **3**(1): p. 33-42.
115. Durocher, D. and S.P. Jackson, *DNA-PK, ATM and ATR as sensors of DNA damage: variations on a theme?* Curr Opin Cell Biol, 2001. **13**(2): p. 225-31.
116. Beuret, L., et al., *BRCA1 is a new MITF target gene*. Pigment Cell Melanoma Res, 2011. **24**(4): p. 725-7.
117. Wu, Z.H., et al., *Molecular linkage between the kinase ATM and NF-kappaB signaling in response to genotoxic stimuli*. Science, 2006. **311**(5764): p. 1141-6.
118. Stokes, M.P., et al., *Profiling of UV-induced ATM/ATR signaling pathways*. Proc Natl Acad Sci U S A, 2007. **104**(50): p. 19855-60.
119. Kim, Y.S., et al., *Phosphorylation of threonine 10 on CKBBP1/SAG/ROC2/Rbx2 by protein kinase CKII promotes the degradation of IkappaBalpha and p27Kip1*. J Biol Chem, 2003. **278**(31): p. 28462-9.
120. Kato, T., Jr., et al., *CK2 Is a C-Terminal IkappaB Kinase Responsible for NF-kappaB Activation during the UV Response*. Mol Cell, 2003. **12**(4): p. 829-39.
121. Bek, S. and R. Kemler, *Protein kinase CKII regulates the interaction of beta-catenin with alpha-catenin and its protein stability*. J Cell Sci, 2002. **115**(Pt 24): p. 4743-53.
122. Bliesath, J., et al., *Combined inhibition of EGFR and CK2 augments the attenuation of PI3K-Akt-mTOR signaling and the killing of cancer cells*. Cancer Lett, 2012. **322**(1): p. 113-8.
123. Silva, A., et al., *PTEN posttranslational inactivation and hyperactivation of the PI3K/Akt pathway sustain primary T cell leukemia viability*. J Clin Invest, 2008. **118**(11): p. 3762-74.
124. Karagiannis, P., et al., *IgG4 subclass antibodies impair antitumor immunity in melanoma*. J Clin Invest, 2013. **123**(4): p. 1457-74.
125. Hensley, C., et al., *In vivo human melanoma cytokine production: inverse correlation of GM-CSF production with tumor depth*. Exp Dermatol, 1998. **7**(6): p. 335-41.
126. Hoffmann, A., T.H. Leung, and D. Baltimore, *Genetic analysis of NF-kappaB/Rel transcription factors defines functional specificities*. EMBO J, 2003. **22**(20): p. 5530-9.

9 EIDESSTATTLICHE ERKLÄRUNG

Hiermit bestätige ich, dass ich die Arbeit selbständig angefertigt habe und andere als die von mir angegebenen Quellen und Hilfsmittel nicht benutzt habe. Die den benutzten Werken wörtlich oder inhaltlich entnommenen Stellen habe ich als solche kenntlich gemacht. Die eingereichte schriftliche Fassung entspricht der auf dem elektronischen Speichermedium.

Hamburg 11.09.2013

Ort, Datum

A handwritten signature in black ink, consisting of a large, stylized 'S' or 'F' shape with a horizontal line through it, positioned above a horizontal line.

Unterschrift

**10 BESTÄTIGUNG DER SPRACHLICHEN KORREKTHEIT DURCH
„NATIVESPEAKER“**

Hiermit erkläre ich die Dissertation von Frau Laia Pagerols Raluy mit dem Titel
**„The functional role of MITF in DNA damage response pathways and its
potential modulation of the immune system by regulating NFkB
phosphorylation“** gelesen zu haben und bestätige ihre Korrektheit in Bezug auf die
Verwendung der englischen Sprache.

Hamburg, September 2013



Lisa Saenz

11 ACKNOWLEDGEMENTS

First of all, I would like to thank Prof. Dr. Martin Horstmann for giving me the opportunity to work in his research group of the 'Kinderkrebs-Zentrum Hamburg'. His support and the freedom he gave me were crucial in developing and finalizing my PhD project. I would also like to express my gratitude to PD Dr. Hartwig Lüthen for accepting the evaluation of my scientific work.

Additionally, I thank all the people in the Kinderkrebs- Zentrum who helped to redirect my ideas with their suggestions, a very special thanks to Anna-Sophie Behlich, Magda Trochimiuk and in particular to Annika Bronsema; I loved our amusing talks about life and science and the great support and encouragement you gave to me. Thank you girls!

I would like to thank my extended family for their interest and support of my work. A special thanks goes out to my mum Carme, my sister Gemma and my friend Tomke for their steadfast emotional support in difficult moments. You are great! Enric and Maria, I heartily thank you for your help, advice and consistency. It was a joy to have you as team! It was also a pleasure to work with Sarah, not only for her technical ability, but also her emotional support. Next, I would like to express my gratitude to PD. Dr. Olaf Hellwinkel and Taylor Saenz for advising and correcting my work; you were a big help in the final stressful moments!

Finally, I thank in heart and soul my husband Marten and my two little girls, Nina and Mila. I am so grateful for having you! I know it was hard to manage these last three years, but we did it! I thank you for your logistic and, above all, emotional support and the encouragement in difficult moments. I love you!